Al-Farabi Kazakh National University

UDC 622.03 (043) Manuscript draft

AIZHULOV DANIAR YERSENOVICH

THE STUDY OF GEOLOGICAL AND HYDROLOGICAL PROCESSES OF ROLL-FRONT TYPE DEPOSITS GENESIS

6D060300 – Mechanics

PhD thesis

Domestic scientific consultant:
Kaltayev Aidarkhan,
Doctor of Physical and Mathematical Sciences, Professor

Foreign scientific consultant
Irina Panfilov
Doctor of physics and mathematics
Head of Engineering and Hydrodynamics of subterrain reservoirs Department of LEMTA
University of Lorrain

Kazakhstan
Almaty, 2024

CONTENTS

NORMATIVE REFERENCES

This dissertation uses references to the following standards:

GOST RK 5.04.034-2011: state obligatory standard of education of the Republic of Kazakhstan. Postgraduate education. Doctorate. Basic provisions (changes dated August 23, 2012 No. 1080);

GOST 7.32-2001. Research report. Structure and rules of registration;

GOST 7.1-2003. Bibliographic record. Bibliographic description. General requirements and rules for compilation.

INTRODUCTION

The relevance of the work. According to World Nuclear Association, Kazakhstan is the 2nd largest country by uranium reserves, accounting for as much as 12% of World's uranium resources. Approximately 40% of all uranium produced in the World can be attributed to Kazakhstan [1]. This has been achieved through the application of so called In-Situ Leaching (ISL) method – an effective, safe technique implemented predominantly for permeable, sandstone mineral deposits [2].

The prices of uranium have been under stress decreasing since 2008, with a recovery observed since late 2020. Major dips can be attributed to the nuclear disarmament procedures, decommission of nuclear power plants and Fukushima nuclear disaster in 2011 [2]. The decline in investments for exploring uranium deposits has been consistent since 2011, as it directly correlates with the decrease in uranium prices. In the light of falling prices, there is a significant decrease in investments [2] with an increase in exploration costs [3], as well as a decrease in reserves that are profitable for production.

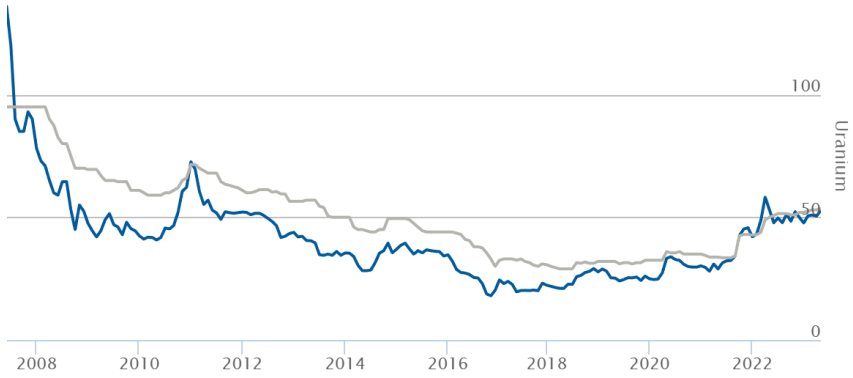

Figure 1 – Change in prices of uranium per pound in a period between 2008 and late 2022 [4]

Furthermore, despite Kazakhstan's second-place ranking in terms of global uranium reserves, there are significant issues concerning its raw uranium supply, majority of which were explored prior to the 1990s. Uranium is one of those resources where extraction volumes greatly exceed new discoveries through exploration. Until now, Kazakhstan has focused on developing deposits with a cost-effective uranium concentration (less than $80 per kilogram), however, over the past years, the number of such resources has declined by a 43%, reaching a total of 2.1 million tons. Based on the projected uranium mining capacity, a shortage of cost-effective uranium resources has been anticipated by 2020 [5]. This deficit inevitably results in reduced profitability for the uranium industry in Kazakhstan.

Rollfront deposits are significant for the mining industry, particularly in the uranium sector. These deposits contribute up to 60% of the global uranium production [6], surpassing other recoverable uranium resources found in sandstone environments.

Major regions hosting uranium rich sandstone deposits include the Plateau of Colorado, Wyoming (USA), Texas Coastal Plain (USA), Mali-Nigeria, Czech Cretaceous Plate, Chu-Sarysu, Syr-Daria, and Kyzylkum in Kazakhstan [7]. The IAEA report on World Uranium Deposits [8, 9] identifies several rollfront deposits, namely Moynkum, Inkai, and Mynkuduk in Kazakhstan, Crow Butte and Smith Ranch in the USA, and Bukinay, Sugraly, and Uchkuduk in Uzbekistan. Kazakhstan, holding nearly a million tons of recoverable uranium (1Mt U in 2013), ranking as the second-largest country globally in terms of uranium resources, has nearly 70% of its resources being extractable using the ISL method [6].

Roll-front deposits is a mineralization that form at redox fronts in permeable rocks [10]. Effective production of minerals through the ISL depends on a comprehensive analysis of mineral distribution, grade values and overall profitability of the extraction. In other words, the performance of any selected technique of production in terms of cost of drilling and further operation, highly depends on the accuracy of geological exploration techniques. Enhancing the comprehension of reactive transport and chemical processes implicated in the formation of rollfront deposits would lead to safer and more economical utilization of ISL methods for exploiting rollfront deposits.

Rollfront deposits contain various minerals, including rare earth minerals such as selenium, molybdenum, rhenium, vanadium, scandium and yttrium [11]. Simultaneously, the mineral concentration in rollfronts is insufficient for exploitation via conventional methods but well-suited for safe and efficient extraction through the ISL method. The ISL production process involves injecting a leaching solution into the reservoir, dissolving and transporting the valuable component, and then pumping the resulting solution to the surface. At the same time, the process of formation of rollfront deposits consists of the following stages: dissolution of a mineral from rocks by oxygen-containing waters, transfer of a dissolved useful component by groundwater, precipitation as a result of a reduction reaction. Hence, the production process using the ISL method mirrors the formation process of rollfront deposits but occurs in reverse and at orders of magnitude faster rates [12].

Given the declining capital infusion in the mineral sector, the advancement of techniques pertaining to geological exploration of mineral reservoirs will facilitate the sustenance of the resource reservoir at an appropriate level. Enhancing the efficacy of deposit development through comprehensive insights into the geometric distribution and reserves of the mineral will curtail production expenses while incorporating additional resources into the economically viable category.

The efficiency of mineral extraction, in terms of drilling and subsequent operational expenses, relies on the precision in determining the outline (contour) and distribution of mineral content within the reservoir. Currently, the demarcation of economically viable ores in the uranium industry is primarily performed manually, relying on established methodological recommendations [13], or alternatively utilizing geostatistical methods [14]. Nonetheless, these employed techniques fail to consider the hydrodynamic and chemical factors that influence the formation of deposits. Conversely, studying the mechanisms behind rollfront deposit formation, would allow

discerning certain patterns in ore distribution within the reservoir. Consequently, this knowledge can contribute to the development of an enhanced geomodelling method for the ore body, yielding improved accuracy. As a result, several benefits can be attained, including cost reduction in exploration and development by minimizing the number of wells required, increased precision in reserve estimations, and enhanced recovery rates during the production process. Despite the availability of various software applications, which employ conventional geostatistical approaches, they lack the capability to refine models by considering the geohydrochemical factors inherent in rollfront deposits.

Based on the aforementioned considerations, the **goal of the work** is to establish the formation mechanisms of rollfront mineral deposits with the purpose of constructing mathematical and numerical models that accurately depict their formation. Additionally, leveraging the acquired findings, the work aims to devise a new geostatistical method for precise geomodelling and reserve estimation of such formations.

In order to accomplish the objective of this research, the following **tasks** have been outlined:

1) numerical reproduction of an empirical experiment on rollfront formation process;

2) development of an appropriate quantitative model of the formation mechanism of the rollfront that can be applied for various bedded geometries;

3) to propose a technique to produce synthetic deposits, based on numerical simulation of hydrodynamics and chemical kinetics of precipitation/dissolution of mineral complexes during the deposit genesis;

4) to propose a new geostatistical method with some modifications/improvements of conventional algorithms by honoring hydrodynamic constraints that govern fluid flows in ore bearing layers;

5) to test the performance of conventional methods as well as a proposed method in terms of accuracy of resource estimation and geological model generation.

The **objects of the study** are the processes of geological modeling and resource estimation of rollfront mineral deposits.

The **subjects of the study** are:

1) the development of a numerical model of rollfront deposit genesis to understand the influence of various geological, hydrogeological and chemical factors on deposit geometry, spatial distribution and contents of the mineral;

2) creation of a geostatistical method specifically suited for epigenetic deposits formed via the propagation of minerals through the permeable rocks.

Methods of the study are: simulation of the processes of transport, dissolution and precipitation of mineral containing solutions in porous media, as well as geostatistical methods for geomodelling and reserve estimation.

The novelty of the work. Current methods for constructing geological models of infiltration type deposits rarely take into account the hydrodynamic and geochemical processes that influence the formation of such deposits. Moreover, at present, constructing the contour of the ore body and calculating the reserves of uranium

deposits in Kazakhstan is carried out manually based on methodological recommendations developed independently in each of the mining industries [15]. Accordingly, the accuracy of the constructed geological models highly depends on the qualifications of a particular expert and can vary greatly from expert to expert. The original research lies in replicating a laboratory experiment numerically in order to broaden the understanding of rollfront genesis mechanisms from geological, hydrodynamic and chemical perspectives. Additionally, these experiments have contributed to the creation of a quantitative model for the numerical generation of synthetic rollfront deposits to acquire data necessary for verification of various geological modeling techniques or for potential utilization in the training of AI-based technologies, such as Physics-Informed Neural Networks. A novel geostatistical method has been created specifically intended for infiltration type deposits, accounting for the hydrodynamic characteristics inherent in their formation processes. Computational Fluid Dynamics methods within the newly proposed method has led to an increase in the accuracy of current geostatistical approaches when implemented for rollfront deposits. The effectiveness of this method has been substantiated through appropriate verification procedures detailed within the current research.

Scientific provisions submitted for defense:

1) reactive transport simulation employed to investigate the formation of rollfront deposits, facilitating the determination of the relationship between various characteristics and the geometry and content of these deposits;
2) mathematical model and a tool for generating synthetic rollfront fields for verification of geostatistical models;
3) a new geostatistical method, utilizing streamlines, devised to construct a geological 3D model of the deposit with increased accuracy;
4) software tool for geological modeling and reserve estimation of rollfront deposits.

Author's personal contribution. Scientific results submitted for defense were obtained by the author independently, while the formulation of the problem was set by the scientific supervisor. Results published jointly with other authors belong to the authors in equal shares. The results of other authors used in the course of writing the dissertation contain links to the relevant sources.

Reliability and validity of scientific provisions, conclusions and results of the dissertation are determined by the use of fundamental laws of mechanics: the laws of conservation of mass, Darcy's Law and Law of Mass Action when devising a reactive transport model for simulating rollfront formation, Pollock's algorithm for streamline generation to amend traditional geostatistical methods, as well as the use of proven and sufficiently accurate numerical methods of computational fluid dynamics. Reaction rates in the model of rollfront genesis were determined based on laboratory experiment. Filtration parameters from real deposits were used during the verification process.

Theoretical and practical significance of the research. Theoretical significance of the work lies in: creation of reactive transport model of rollfront formation and development of fundamentally new geostatistical method targeted at

geomodelling of infiltration type epigenetic deposits. Based on the laboratory experiment a mathematical reactive transport model has been developed by identifying reaction rate constants in redox environment at the geochemical barrier which results in accumulation and redeposition of minerals containing uranium along with other useful components. The model, not only broadened hydrochemical understanding of formation of such deposits, but also provided a tool for generation of synthetic deposit data, which can be used to verify the effectiveness of any geostatistical approaches or train neural networks. By using conclusions made from reactive transport modeling a new geostatistical method has been developed, by accounting for these deductions. Results show, that by honoring hydrodynamic nature of rollfront deposit genesis, accuracy of geostatistical modeling can be increased.

Connection of the dissertation work with other research works.

Some parts of this dissertation were conducted within the framework of the following projects.

1) BR05236447 "Intelligent control and decision-making systems for the development of uranium and oil deposits" targeted program funding for scientific research from the Ministry of Education and Science of the Republic of Kazakhstan, 2018 – 2020, project number GR 0118RK01275. Some deductions made within the dissertation in regards of mechanisms and geostatistical approaches were used to create a geological interpolation module [16].

2) AP08051929 "The study of the mechanisms of ore genesis and development of high accuracy digital technology to contour ore bodies in rollfront type mineral deposits", grant funding for scientific research from the Ministry of Education and Science of the Republic of Kazakhstan, 2020-2022, project number GR 0120PK00058. Results of the study conducted within the dissertation work were used in order to develop a high precision tool of contouring the ore body of infiltration-type deposits [17].

3) AP09260105 "Development of mathematical foundations and 3D simulation model of the process of underground bacterial leaching of uranium", grant funding for scientific research from the Ministry of Education and Science of the Republic of Kazakhstan, 2021-2023. Research findings obtained through the research work conducted within this dissertation were used as prerequisites for modeling of In-Situ Bacterial Leaching [18].

Approbation of work. Author of current dissertation has collaborated with subsidiaries of National Atomic Company JSC Kazatomprom to develop a large geotechnological programming complex to simulate processes of In-Situ Leaching within a framework of various projects. Results of the research were used to develop a geological software module to interpolate log data from exploration and technological wells to construct a geological and mineralogical model, necessary for effective production of uranium. Software modules were deployed into various entities including LLP "Mining Company Ortalyk", JV Inkai LLP and "Institute of Hight Technology" LLP, all subsidiaries of JSC Kazatomprom, a largest company by uranium production in the world (as of 2024).

Publications. Author has published 16 works, including in 2 indexed in Scpous and/or Web of Science databases [9, 19], in 2 journals recommended by Science and Higher Education Quality Assurance Committee of the Ministry of Science and Higher Education of the Republic of Kazakhstan [20, 21], as well within various conferences and symposiums. Notable conferences include specialized conference held by JSC Kazatomprom [22] and International Symposium on Uranium Raw Material for the Nuclear Fuel Cycle: Exploration, Mining, Production, Supply and Demand, Economics and Environmental Issues (URAM-2018) [23]. Results of the research were used to develop several software modules, for which 10 copyright certificates were obtained.

Thesis structure and scope. The dissertation thesis consists of an introduction, two chapters, a conclusion, bibliography, and appendices. The work is presented on 52 pages and contains 35 figures.

The main content of the dissertation. The dissertations consist of two main chapters.

Chapter 1 “Quantitative model of the formation mechanism of the rollfront uranium deposits” aims at aims numerical replication of the laboratory experiments through reactive flow and numerical simulation techniques. A proper definition of rollfront deposit is made in this chapter. Geometry, content, mechanisms of formation as well as other its chemical and physical properties are discussed. Derived quantitative model allows the identification of the factors responsible for the formation of crescent-like structures and the determination of the key mechanisms influencing rollfront evolution. The results of this chapter were published in [9] as well as presented at numerous conferences” including [22-24].

The research results provided in Chapter 2 “Development of streamlines based stochastic method for resource estimation of rollfront deposits” explores using stochastic simulations to understand ore grade distribution in rollfront deposits and the geological processes involved. A geostatistical algorithm to better capture hydrodynamic constraints governing fluid flows is suggested. One proposed improvement involves incorporating so called time of flight (TOF) of water particles along streamlines when calculating variograms, departing from traditional distance-based metrics. This approach aims for more accurate interpolation and resource estimation. Non-deterministic streamline-based methods offer promise for improved results compared to traditional geostatistical approaches, particularly for roll-front deposits, by better addressing fluid flow characteristics and constraints. The results of this chapter were published in [19] as well as presented at numerous conferences” [22-24].

1 QUANTITATIVE MODEL OF THE FORMATION MECHANISM OF THE ROLLFRONT URANIUM DEPOSITS

Rollfront type deposits are characterized by crescent-shaped accumulations of mineralization, including uranium, selenium, and molybdenum, within permeable sandstones [11]. These deposits typically contain a so-called geochemical barrier between reduced and oxidized environments. The interplay of redox reactions between oxidants and reductants creates favorable conditions for uranium precipitation, while a continuous influx of oxidants leads to the dissolution of uranium minerals, resulting in reactive transport [25]. Previous research has predominantly focused either on the characteristics of rollfront type deposits or on describing the chemical and geological processes involved in their formation.

This chapter aims to numerically replicate laboratory experiments through reactive flow and numerical simulation techniques. Data from a specific experiment were utilized to determine reaction rates between reactants, resulting in the development of a model that encompasses reactive transport and chemical processes relevant to the formation of rollfront type deposits. This model facilitates the identification of the factors responsible for the formation of crescent-like structures and the determination of the key mechanisms influencing rollfront evolution. By attaining a better understanding and simulation of the mechanisms governing the formation and properties of rollfront type deposits, exploration and production costs associated with these accumulations can be reduced. Furthermore, the findings of this study have broader applicability in modeling other deposits formed through the infiltration and subsequent precipitation of various minerals at the redox interface.

Rollfront deposits encompass a variety of minerals, but particular emphasis is placed on rollfront uranium deposits, given their significant importance to the uranium industry in Kazakhstan.

1.1 The process of rollfront genesis

According to some definitions [10-12], rollfront uranium deposits, also known as stratum infiltration-type or stratum oxidation deposits, are described as accumulations of uranium (U), selenium (Se), and molybdenum (Mo) compunds within reduced permeable sediments, primarily sandstones. These deposits form along the boundary, known as the rollfront or geochemical barrier, between predominantly reduced and extensively oxidized environments. In terms of spatial geometry, rollfront deposits are described by the International Atomic Energy Agency as "zones of uranium-matrix impregnations that intersect sandstone bedding and extend vertically between less-permeable horizons above and below" [26]. In his extensive work, Dahlkamp [27] outlines the following properties associated with rollfront deposits: they exhibit elongated and sinuous shapes when viewed from above, with lines perpendicular to the direction of groundwater flow; the mineralization zones have a vertically convex configuration; they possess diffusive boundaries with reduced sandstone in downstream part of the groundwater flow and distinct contacts with oxidized sandstone in upstream part of the groundwater flow. Rollfront deposits are

sedimentary and epigenetic, indicating they formed after the host environment. These deposits are found in arid regions and are restricted to permeable geological formations.

In her study, Maksimova [11] extensively examined the key factors contributing to the formation of polyelement (uranium, molybdenum, selenium, rhenium, vanadium, scandium, yttrium, lanthanides) rollfront deposits, which are primarily found within aquifers of the sedimentary cover. Through a comprehensive analysis of hydrodynamic data, the research provided a detailed characterization of the bedded epigenetic zonality that controls the mineralization and elucidated the behavior of various chemical elements during the ore-forming process. Significantly, the study established that the hydrodynamic factor plays a crucial role in the formation of rollfront deposits. Consequently, it was concluded that rollfront deposits can only form within artesian basins that have an infiltration hydrodynamic regime.

Dahlkamp's works [27, 28] provide a comprehensive overview of the geological structure of uranium deposits, offering a typological classification accompanied by detailed descriptions of individual uranium regions and deposits. These publications encompass a range of deposit types and examine their specific formation characteristics, including epigenetic occurrences. Notably, in [28], Dahlkamp highlights the distinctive features of rollfront deposits, which are delineated as arcuate zones comprising uranium matrix inclusions, confined by impermeable horizons above and below. The mineralized zones exhibit elongated and sinuous bands aligned along permeable layers and perpendicular to the groundwater flow. Down the hydrological gradient, the mineralized zones assume a convex shape, usually described as a form of “elongated tongue” in Soviet litareture. They display diffuse boundaries with reclaimed sandstone downstream of the water table, while sharply demarcated boundaries are observed with oxidized sandstone upstream as shown in Figure 2.

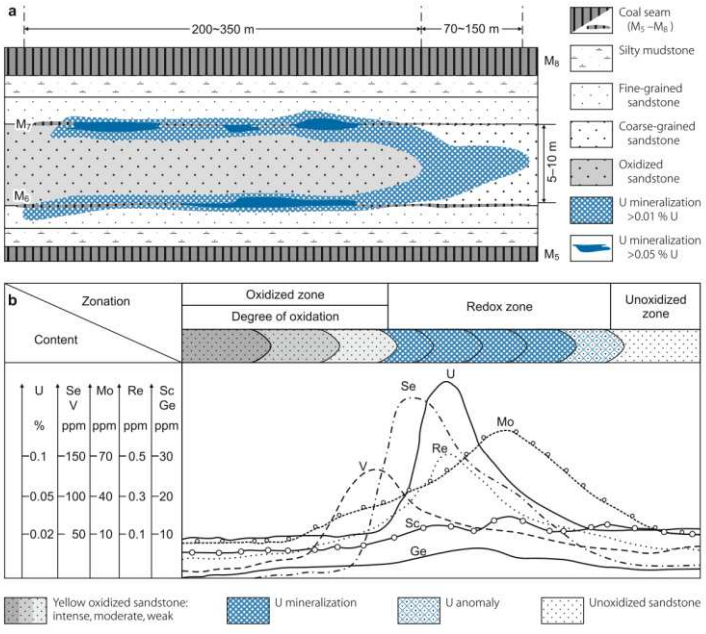

Figure 2 – An example of rollfront deposit as seen in vertical section (a) along with typical distribution of various compounds (b) [27]

The publication also sheds light on the geographical and geometric attributes of the mineralization. Uranium is found within sandy horizons, spanning depth intervals ranging from 80 meters to over 500 meters. These horizons extend along highly stretched mineralized zones, spanning for hundreds of kilometers, characterized by intricate redox fronts. Certain sections of these zones are delineated as deposits based on arbitrary criteria. Ore bodies associated with redox fronts primarily manifest as rolls. When observed in a plane view, the rollfront ore bodies exhibit continuous, meandering belts, ranging from several kilometers to 30 kilometers in length and 20 to 1,000 meters in width. In cross-section, they typically possess an asymmetric crescent shape, with a thickness of 1 to 30 meters and variable-length tails. For Southern Kazakhtsan deposits the ore formation began with the uplift of the Tien Shan ranges. Indirect evidence suggests that the Tien Shan Mountains, adjacent to the Chu-Sarysu basin from the south and southeast, not only supplied rollfronts with sediments, but also provided uranium and other ore-related elements.

In Yazikov's study [29], an inventory of hydrogeological factors that impact the economic attractiveness of rollfront deposit production is identified, encompassing various aspects. These factors include the lithological composition and thickness of water-bearing rocks, the depths of aquifers and groundwater levels, the characteristics of groundwater development, the direction and velocity of natural groundwater flow, the presence of underlying and obstructing aquicludes, as well as the filtration properties of the rocks in the ore-bearing horizon. These hydrogeological factors play a significant role in determining the economic viability of rollfront deposit extraction.

The work [30] comment on the patterns and timeframes associated with the formation and location of uranium deposits. Within the study, several subtypes of deposits are identified, including roll deposits characterized by oxidation fronts in reservoirs, commonly known as rollfront deposits; startum oxidation deposits; near-fault-stratal deposits, and paleovalley deposits. These distinct subtypes contribute to a comprehensive understanding of uranium deposit diversity and formation processes.

Various hydrodynamic groundwater regimes [7] play a crucial role in the formation of uranium mineralization. The groundwater is primarily influenced by surface topography and governed by gravitational forces. Important factors in genesis of the deposit are the permeability of the hosting rocks and presence of a redox barrier within the zone. The water regime, in conjunction with the rock composition, significantly influences the morphology of ore bodies as well as the texture and structure of the ores.

Another study [31] examines the patterns governing the spatial distribution of uranium and explores the factors that contribute to the formation of substantial deposits. The research proposes a model for estimating potential resources, which takes into account several key factors. These factors include the initial and residual uranium content in solutions, rock permeability, hydraulic slope, duration of ore formation, and the degree of contrast in the reduction barrier. By considering these factors, a comprehensive assessment of potential resources can be achieved.

Following a review of studies investigating hydrodynamic and hydrogeological processes involved in the formation of rollfront deposits, the following factors were considered:

1) Gravity is the basis of the movement of groundwater, and the flow within the reservoir is due to the presence of a hydraulic gradient;

2) filtration properties affect the final geometry of the ore body;

3) rollfront deposits usually have upper and lower impermeable beddings;

4) in top view, the eventual form of mineralization appears as a sinusoidal ribbon (as seen in Figure 3), while in vertical section, it resembles a crescent or elongated tongue.

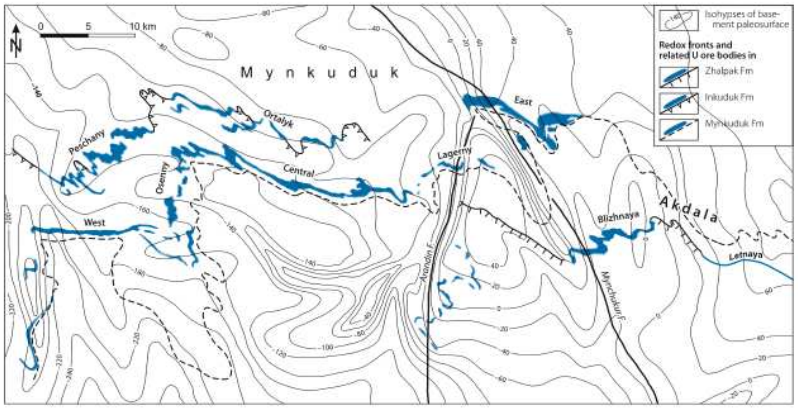

Figure 3 – An example of Mynkudyk deposit, featureing the sinusoidal shape of a typical rollfront as seen from top view (courtesy Dahlkamp [27])

The genesis of rollfront type deposits involves three primary stages (Figure 4): a leaching phase caused by oxygenated meteoritic water dissolving minerals from mountain rocks, followed by the migration of dissolved chemical components, and ultimately, the end deposition of useful compounds. In the case of the Tianshian mega-province (Chu-Sarysu and Syrdaria basins) in southern Kazakhstan, which hosts a substantial amount of uranium [7], uranium-enriched minerals like zircons, monazites, and accessory minerals were leached by oxygen-rich rainwater from the granitic Tianshian Mountains. These minerals were subsequently transported downstream through porous, unconsolidated sandstones. Upon reaching reduced environments, the dissolved uranium, along with other elements such as iron and sulfur, precipitated as uranium minerals primarily in form of pitchblende and coffinite in Kazakhstan's uranium deposits, as well as pyrite (FeS_2), resulting in the formation of a rollfront type deposit. It is noteworthy that the redeposition of minerals is a dynamic process of dissolution and precipitation, sustained by a continuous flow of oxygenated water that "pushes" minerals further downstream. In active deposits, minerals continuously dissolve from the upstream side of the mineralization zone and precipitate at the further side of the rollfront. When the water flow no longer contains sufficient oxygen, often due to prior consumption through the oxidation of organic matter before reaching the mineralized zone, the rollfront stabilizes.

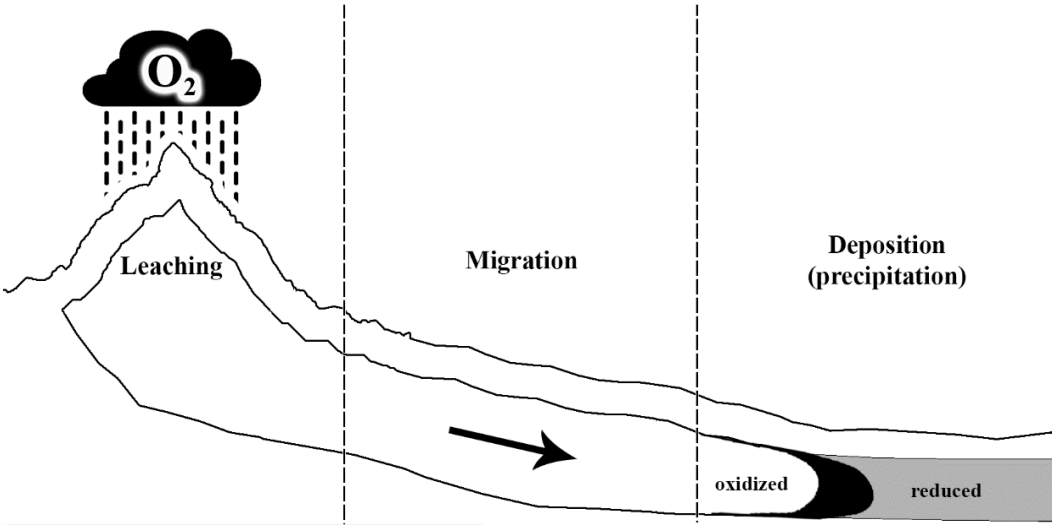

Figure 4 - Schematic representation of stages of the genesis of rollfront deposits

Evidently, the precipitation and dissolution of uranium can involve complex chemical interactions. The limited understanding of the specific chemical compounds, involved in the reactive transport process during the time of genesis, poses a significant challenge in modeling the formation of rollfront deposits. Furthermore, factors such as temperature, pressure, Eh (redox potential), and pH influence uranium precipitation pattern. Lower oxidation levels and higher pH values both contribute to the formation of precipitated minerals [11].

Some literature sources [11, 32] contain extensive information on the mineralogy of uranium minerals. Numerous uranyl and uranous complexes can form with various anions, including sulfates (UO_2SO_4,USO_4^{2+}), carbonates ($UO_2(CO_3)_2^{2-}$,UO_2CO_3), phosphates (UO_2HPO_4,$UO_2(HPO_4)_2^{2-}$), chlorides (UCl^{3+},UO_2Cl^{+}) or fluorides (UO_2F^{+},UF^{3+}). Assuming that, uranium migrates in oxygenated aquifers mostly as carbonate anions ($UO_2(CO_3)_3^{4-}$, or $UO_2(CO_3)_2^{2-}$), the general scheme for uranium precipitation upon reaching reduced environment can be written as follows [11]:

$$UO_2(CO_3)_{2(dis)}^{2-} + 2e^- \rightarrow UO_{2(crystal)} + 3CO_{3(dis)}^{2-} \quad (1)$$

In a reduced environment, substances like pyrite and organic matter serve as electron donors, playing a crucial role in facilitating the precipitation of uranium. When oxygenated waters interact with a reduced environment, they form a geochemical barrier that fosters favorable conditions for uranium precipitation, such as pyrite being able to provide electrons to the environment by oxidizing the iron that switches its oxidation state from ferrous Fe^{+2} to ferric Fe^{+3} and releasing SO_4^{2-} sulfate ion into the water:

$$FeS_{2_{(crystal)}} + 3.5O_2 + H_2O \leftrightarrow Fe^{2+}_{(dis)} + 2SO^{2-}_{4_{(dis)}} + 2H^+ \quad (2)$$

Oxygenated waters have the ability to convert precipitated uranium minerals back into a dissolved form. The dissolution reaction involves the conversion of crystallized uranyl dioxide back into uranyl carbonate and can be represented by the following chemical half-reaction:

$$UO_{2_{(crystal)}} + 3CO^{2-}_{3_{(dis)}} \rightarrow UO_2(CO_3)^{2-}_{2_{(dis)}} + 2e^- \quad (3)$$

Similar schemes are available for other minerals. For instance, selenium migrates within oxygenated groundwater, predominantly in the form of hydroselenite ions $HSeO_3^{2-}$ and selenite ions SeO_3^{2-}. The zone of reductive deposition of native selenium can be determined through the following half-reaction equations:

$$\begin{aligned} &HSeO^-_{3\ (dis)} + 5H^+_{dis} + 4e^- \leftrightarrow Se_{(cryst)} + 3H_2O_{(dis)} \\ &SeO^-_{2\ (dis)} + 6H^+_{(dis)} + 4e^- \leftrightarrow Se_{(cryst)} + 3H_2O_{(dis)} \end{aligned} \quad (4)$$

Both laboratory and field experiments have validated that selenium can be extracted concurrently with uranium through sulfuric acid leaching, utilizing leaching methods, given the introduction of oxidizing agents.

In the majority of infiltration deposits found in rocks containing carbonaceous organic matter or epigenetic reducing agents, rhenium forms ore accumulations. Typically present in concentrations ranging from tenths of grams per ton, rhenium is delineated within a roll-shaped body often associated with uranium ore rolls. Within formation-filtration ores, rhenium primarily exists in mineral forms such as oxides and sulfides. The reductive precipitation of this valuable component can be described by the following half-reaction.

$$\begin{aligned} 2\,Re\,O^-_{4\ (dis)} + 2S_{(cryst)} + 12H^+_{dis} + 10e^- \\ \leftrightarrow Re\,O_{2(cryst)} + Re\,S_{2(cryst)} + 6H_2O_{(dis)} \end{aligned} \quad (5)$$

Rhenium is extracted from ores using the ISL method, employing either the acid or bicarbonate scheme. In the absence of an oxidizing agent, the concentration of rhenium ranges from 0.08 to 0.4 mg/l, while with the addition of an oxidizing agent, the concentration ranges from 0.2 to 0.7 mg/l.

The migration of vanadium in an oxidizing environment primarily occurs in the form of the dissociate of orthovanadic acid, $H_2VO_4^-$. Its mobility is predominantly constrained by uranium due to the low concentration of uranyl vanadates. The involvement of vanadium in the oxidation process of formation-infiltration is primarily driven by an increase in the alkalinity of the hydrogeochemical medium. As the front part of the oxidation zone is reached, characterized by acidification of the medium, the vanadate ion can combine with the uranyl ion, resulting in the formation of ore

carnotite-tiamunite seam-infiltration mineralization. This process can be described by the following half-reaction:

$$2UO_2(CO_3)^{4-}_{3\,(dis)} + H_2VO^-_{4(cryst)} + 2K^+_{dis} + 3H_2O_{(dis)} + 2H^+_{(dis)} \leftrightarrow \\ \leftrightarrow K_2(UO_2)_2(VO_4)_2 \cdot 3H_2O_{(cryst)} + HCO^-{}_{3(dis)} \quad (6)$$

1.2 Numerical reproduction of an empirical experiment

To develop a mathematical model for simulating rollfront genesis, author has utilized a suitable laboratory experiment as a reference. Evseeva et al. [33] conducted an experiment in a laboratory setting to simulate the formation of uranium rollfront deposits. In the experiment, Evseeva employed a transparent plastic box measuring 2 × 0.15 × 0.2 m (Figure 5). Initially filled with sand, the plastic box underwent several chemical manipulations, converting the iron oxide within it into sulfides, thus establishing a reduced environment. Following this, water with uranium concentrations ranging from approximately 10^{-6} to 10^{-5} g·l^{-1} was passed through the box, leading to the development of a roll-shaped accumulation of uranium.

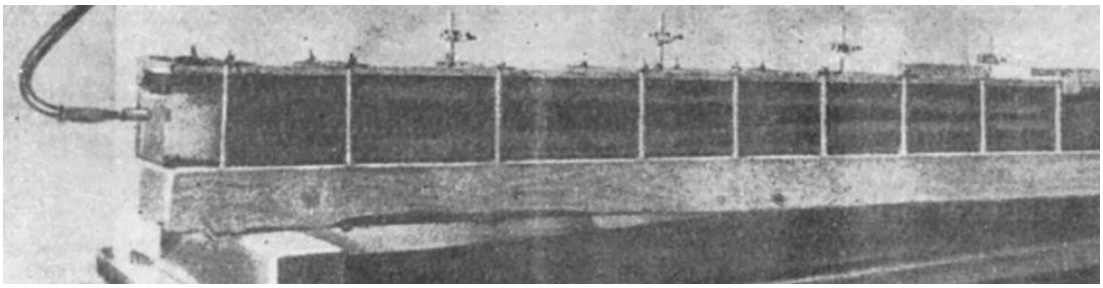

Figure 5 – A photo of a glass box used by Evseeva in her empirical experiment to reproduce the formation of rollfronts in a laboratory setting [33].

The resulting distribution of uranium in the box, characterized by a consistent increase in uranium concentration and the migration of the oxidation zone into the reduced sands, successfully replicated the roll-like accumulations of uranium in the laboratory experiment; however, the mechanisms responsible for such shapes were not adequately explained at the time.

Considering the porous nature of the medium in which rollfront deposits form, the definitive diffusion and extension of a deposit "tongue" cannot be comprehensively explained without considering slip boundary conditions for the viscous flow [9]. Therefore, other factors must contribute to the formation of the crescent-shaped mineralization.

The predominant chemical process observed within the experimental setup involved redox reactions. Despite this, there was limited re-deposition of uranium, which can be attributed to the presence of low oxidizer concentrations and/or inadequate durations for the dissolution and mobilization of uranium. Consequently, uranium concentrations exhibited a decreasing trend along the length of the container, indicating higher initial concentrations near the inlet.

Drawing upon existing data, the subsequent goals of this investigation encompassed identifying the factors contributing to the formation of crescent-like structures and obtaining the principal mechanisms shaping the development of rollfront deposits.

Several assumptions were requisite for the execution of a numerical experiment. Primarily, it was assumed that the solution, and by extension, all fluids within the domain, are incompressible, with reagent flow taking place within the water. The diffusive transport of the mineral exhibits a notably lower rate in comparison to convective transport. Initially, the concentration of reductant is abundant, surpassing that of other reagents by a significant margin. The concentration of oxidant utilized in the experiment should be maintained at a low level, approximately 0.001 gram per liter, similarly to the oxygen concentrations typically encountered in groundwater within Central Asian deposits.

1) the fluids within the box are assumed to be incompressible, and the movement of reagents occurs within the water;

2) the diffusive transport of the mineral is significantly lower compared to convective transport;

3) the amount of reductant present is much higher than that of other reagents;

4) the concentration of oxidant used in the experiment was kept low, approximately 0.001 gram per liter, which is similar to the oxygen concentrations found in groundwater in Central Asia deposits [11].

All the aforementioned processes represent the filtration of concentrations through a porous medium. Hence, Darcy's Law served as a fundamental basis for modeling the hydrodynamics. Mass conservation is described as:

$$div\,\vec{u} = 0 \tag{7}$$

where $\vec{u}$ is flow velocity ($m \cdot s^{-1}$).

Flow velocity within porous medium can be described as:

$$\vec{u} = -\frac{K}{\mu} grad\ p \tag{8}$$

where

K – permeability of the porous medium [m^2],

μ – dynamic viscosity [Pa·s].

Gulberg-Waage's Law of Mass Action, a foundational principle in chemical equilibrium, describes the interplay between various chemical species when a system reaches equilibrium. It has been extensively used to model phenomena of transport in porous medium [34], as well as to simulate reactive transport specifically in the context of uranium production with In-Situ techniques [35]. It asserts that the rate of a chemical reaction is directly proportional to the product of the concentrations of the reactants, each raised to the power of their respective stoichiometric coefficients. This law provides a quantitative framework for understanding how reactions proceed

towards equilibrium and helps predict the composition of the equilibrium mixture based on initial conditions and reaction parameters. For instance, the reaction rate between two reagents A and B can be represented by the equation kC_AC_B, where k denotes the temperature-pressure-dependent reaction constant, and C_AC_B represents the concentration (which is proportional to the collision probability of particles).

For numerical modeling to replicate Evseeva's laboratory experiment, a 2D domain was employed, featuring an inlet on the left and an outlet on the right as shown on Figure 6.

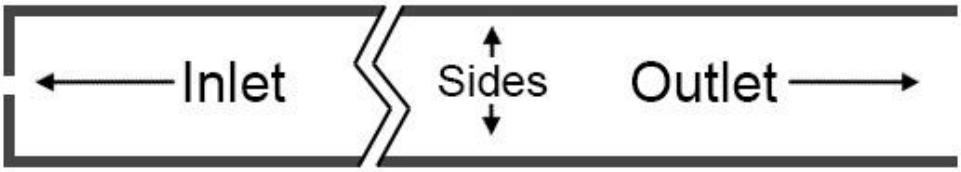

Figure 6 – Schematic depiction of the computational domain for numerical analysis

Using the aforementioned principles of rollfront formation and the insights gained from the laboratory experiment, a numerical simulation was conducted to replicate the following scenario. A porous medium with a high concentration of a reductant, was placed inside a box. Over a duration of 60 days, a constant inflow of water containing dissolved uranium and an oxidant was introduced through an inlet. The redox reaction between the reductant and oxidant was simplified using the following scheme:

$$\begin{cases} reducer + oxidant \xrightarrow{k_1} electrons + product \\ electrons + product \xrightarrow{k_2} reducer + oxidant \end{cases} \quad (9)$$

Electron bearing elements concentration and additional product concentration are a result of reductant oxidation.

Electron-bearing elements play a role in the process of converting dissolved uranium into a solid form, where the concentrations of dissolved uranium and solid uranium are considered in the model. As previously mentioned, in natural conditions, minerals can be redeposited by oxygenated waters through the dissolution of solid complexes. Hence, the precipitation and dissolution of uranium minerals can be represented by the following simplified scheme:

$$\begin{cases} dissolved\ mineral + electrons \xrightarrow{k_3} solid\ mineral \\ solid\ mineral + oxidant \xrightarrow{k_4} dissolved\ mineral \end{cases} \quad (10)$$

The equation that describes the change in reductant concentration is based on the Law of Mass Action and can be expressed as follows:

$$\frac{\partial C_{red}}{\partial t} = \frac{k_2 C_e C_{pr} - k_1 C_{red} C_{ox}}{(1-\theta)\rho_{solid}} \tag{11}$$

where
C_{red} – reduced environment concentration [g·l^{-1}],
C_e – electron bearing elements concentration [g·l^{-1}],
C_{pr} – product of reductant oxidation concertation [g·l^{-1}],
C_{ox} – oxidizer concentration [g·l-1],
k – reaction constant for each reaction,
t – time [sec],
θ – porosity,
ρ_{solid} – density of solids [kg·m^{-3}].

In other words, the decrease in the concentration of the reductant is directly proportional to the inflow of oxidant and inversely proportional to the concentration of redox products. Similarly, the concentration of oxidant is consumed during the oxidation of solid uranium complexes and the reaction with the reductant, and can be mathematically described by the following equation:

$$\frac{\partial C_{ox}}{\partial t} + \vec{u} \cdot grad C_{ox} = \frac{k_2 C_e C_{pr} - k_1 C_{red} C_{ox} - k_4 C_{sol} C_{ox}}{\theta \rho_{liquid}} \tag{12}$$

where
C_{sol} - precipitated solid mineral concentration [g·l-1],
$\vec{u}$ – solution flow velocity [m·sec^{-1}],
ρ_{liquid} – density of liquids [kg·m^{-3}].

The equation includes a convective term ($\vec{u} \cdot grad C_{ox}$) to account for the oxidant being in the dissolved phase. The changes in the concentration of the redox product and electrons can be described by the following equations respectively:

$$\begin{gathered} \frac{\partial C_{pr}}{\partial t} + \vec{u} \cdot grad C_{pr} = \frac{k_1 C_{red} C_{ox} - k_2 C_e C_{pr}}{\theta \rho_{liquid}} \\ \frac{\partial C_e}{\partial t} + \vec{u} \cdot grad C_e = \frac{k_1 C_{red} C_{ox} - k_2 C_e C_{pr} - k_3 C_e C_{dis}}{\theta \rho_{liquid}} \end{gathered} \tag{13}$$

The concentration of electrons is the main factor involved in the dissolution of uranium and can be described by following equation:

$$\frac{\partial C_{dis}}{\partial t} + \vec{u} \cdot grad C_{dis} = \frac{k_4 C_{sol} C_{ox} - k_3 C_{dis} C_e}{\theta \rho_{liquid}} \tag{14}$$

The inflow of oxidant is described as a main factor influencing uranium crystallization:

$$\frac{\partial C_{sol}}{\partial t} = \frac{k_3 C_e C_{dis} - k_4 C_{sol} C_{ox}}{(1-\theta)\rho_{solid}} \tag{15}$$

The numerical experiment employed boundary conditions that were consistent with those used in the laboratory experiment conducted by Evseeva et al. [33]. Specifically, the outlet of the system was subjected to an atmospheric pressure p [Pa] boundary condition:

$$p|outlet = p_{atm} \tag{16}$$

At the inlet, a constant boundary condition is applied to the flow velocity, specifically set at 1.44 10-4 m·s^{-1} at the inlet, which corresponds to:

$$p|inlet = p_{atm} + \rho g h \tag{17}$$

The variable h represents the height equal to 0.74 meters. Except for the inlet and outlet, a no-flow boundary condition is applied to all solid sides of the box:

$$\vec{u} \cdot \vec{n}|_{sides} = 0 \quad \text{or} \quad \frac{\partial p}{\partial n}|sides = 0 \tag{18}$$

Corresponding to the fact that only dissolved uranium is injected into the system, the boundary conditions for all concentrations in the liquid phase adhere to the following conditions (expressed in grams per liter):

$$\begin{gathered} C_{dis}|_{inlet} = 7.5 \cdot 10^{-5}, C_{ox}|_{inlet} = 0.002, C_e|_{inlet} = 0, C_{pr}|_{inlet} = 0 \\ \frac{\partial C_{dis}}{\partial n}|_{sides} = 0, \frac{\partial C_{ox}}{\partial n}|_{sides} = 0, \frac{\partial C_e}{\partial n}|_{sides} = 0, \frac{\partial C_{pr}}{\partial n}|_{sides} = 0 \end{gathered} \tag{19}$$

The initial concentrations of the liquids are:

$$C_{dis}|_{t=0}, C_{ox}|_{t=0} = 0, C_e|_{t=0} = 0, C_{pr}|_{t=0} = 0 \tag{20}$$

Concentrations of solids have the following initial conditions:

$$C_{sol}|_{t=0} = 0, C_{red}|_{t=0} = 1 \tag{21}$$

Prior to the initiation of the inflow, the box was devoid of uranium and contained a reduced porous medium consisting of sand and ferrous iron.

According to the model, the formation of solid uranium is exclusively attributed to a precipitation reaction. Obtaining an analytical solution for the system of differential equations considering the given boundary and initial conditions proves to be a challenging task. Consequently, numerical solutions were obtained using the

COMSOL Multiphysics software, followed by a development of a simulation software using C#.NET.

1.2 Results of the numerical reproduction of an empirical experiment

Upon numerous adjustments of the reaction rates through a trial-and-error process, the results obtained from the numerical simulation began to align with the experimental data (refer to Figure 7). The reason behind the higher uranium concentrations observed at the initial section of the box is likely attributed to the relatively slow oxidation rate of the uranium minerals compared to the flow velocity. Although some of the solid minerals were redeposited within the given short timeframe, as depicted in Figure 7, leading to an increase in the maximum concentration up to 0.015 $g \cdot l^{-1}$ at a distance of 15 cm from the inlet. Similar to the experimental observations, only insignificant amounts of the reducer were leached and transported further away from the inlet. The presence of oxidized reductant is clearly visible in both the laboratory experiment and the results of the numerical simulations.

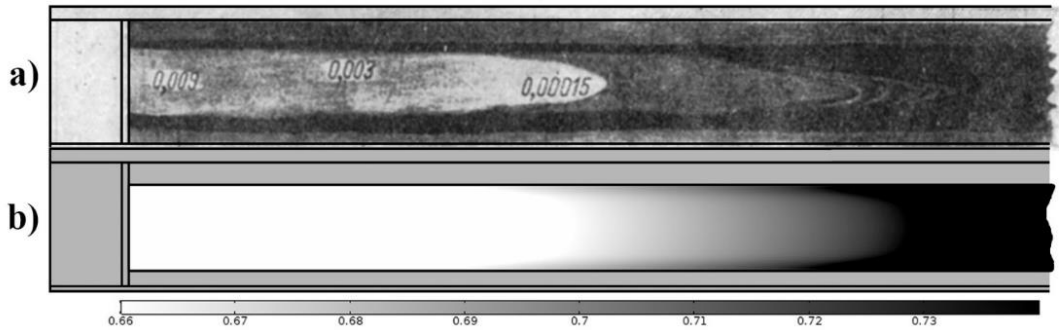

Figure 7 – The change in oxidation state comparison: a) Experimental results showing the observed reductant concentration along the box [33]. b) dissolution of the reductant inside the domain as obtained by numerical simulation

The numerical approach yielded results that started to align with the experimental data as seen on Figure 8 when the reduction reaction rates were substantially greater than the oxidation reaction rates. This indicates that the concentration of the reducer was higher than that of the oxidant.

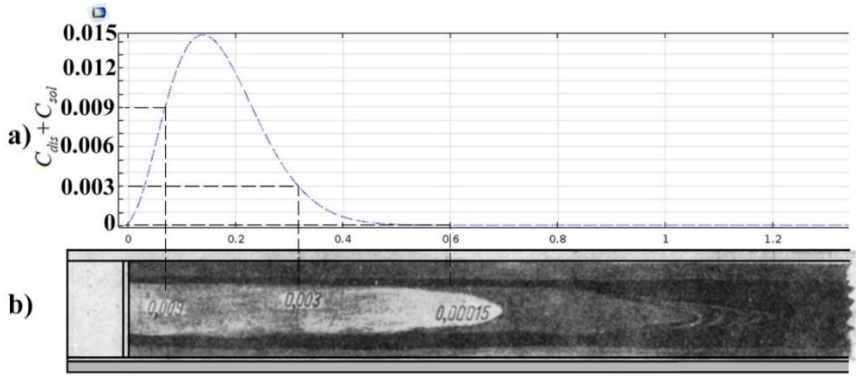

Figure 8 – The total concentration of uranium, both solid and dissolved in [g/l] over the distance in [m] from the inlet of the box obtained from the numerical modeling as compared to the laboratory experiment

After successfully matching the laboratory experiment, the numerical simulation was extended to observe the appearance of crescent-shaped rollfront concentrations over a longer period. The simulation, depicted in Figure 9, spanned 3,300 days with an inflow velocity of 10^{-4} m·s^{-1}. Apparently, the rollfront maintained its shape and moved approximately 15 meters along the liquid flow.

It is worth noting that despite the absence of convection or diffusion terms in the solid uranium concentration equation, the rollfront exhibited a gradual shift over time, as shown in Figure 9. This displacement is a result of the dissolution and precipitation chemical reactions that took place in the domain. During this process, the reductant is leached and redeposited along with the uranium minerals, while some of its concentration is consumed in order to reduce the dissolved uranium.

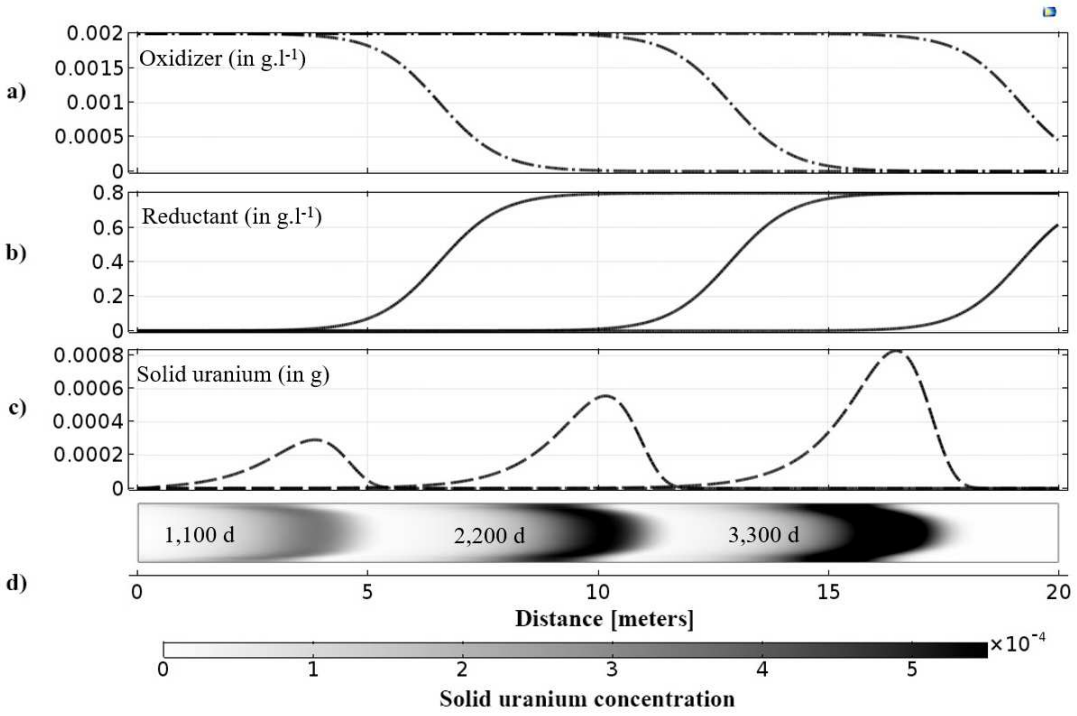

Figure 9 – Re-deposition of uranium solid mineral observed over the periods of 3,300 days with a) oxidizer concentration; b) reductant concentration; c) solid uranium concentration. d) solid uranium concentration visualization in 2D

It is important to highlight the presence of a small radial structure in the velocity field near the inlet point, which is observed in both the laboratory and numerical experiments. This non-parallel flow pattern at the inlet is likely responsible for the formation of the crescent-shaped uranium deposition, as depicted in Figure 10. The flow within the box exhibits higher velocities in the middle compared to the edges, indicating a non-uniform inlet flow.

However, as the flow progresses further into the box, it eventually stabilizes into a parallel flow regime. This observation suggests that the slowdown of the flow along the edges is not solely attributed to the viscosity of the fluid.

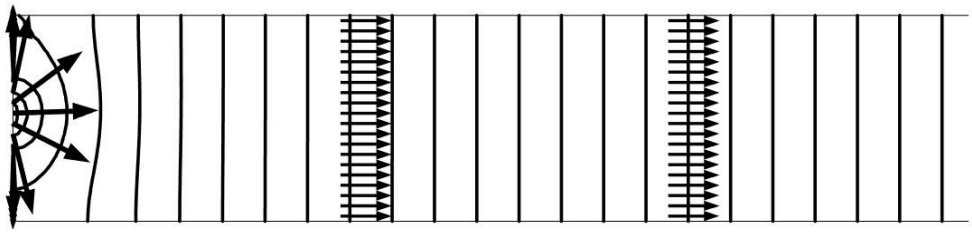

Figure 10 – Velocity field visualized for the domain in use

In order to verify this hypothesis, the boundary conditions were modified to eliminate the narrowing effect in the inflow. Upon recalculating the model with the redesigned boundary conditions, the results revealed a straight front, as shown in Figure 11. This indicates that the formation of the rollfront shape is influenced by the non-uniform distribution of the inlet velocity flow within the system.

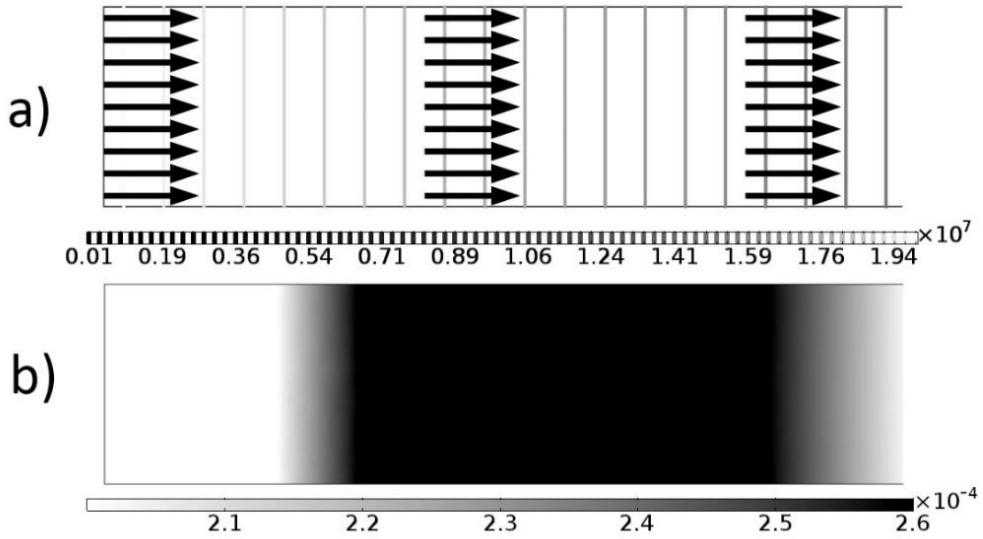

Figure 11 – Numerical results for a non-constricted, non-expanding channel: a) velocity indicated by arrows and pressure indicated by vertical lines, b) shape of a rollfront deposit in a 2D vertical section.

Hence, based on these numerical simulations, it can be inferred that the roll-like shapes are formed as a result of channel constriction, which leads to an increase in flow velocity and subsequent changes in the pressure gradient. To explore this phenomenon further, additional numerical experiments were carried out, incorporating various levels of channel constriction, as depicted in Figure 12.

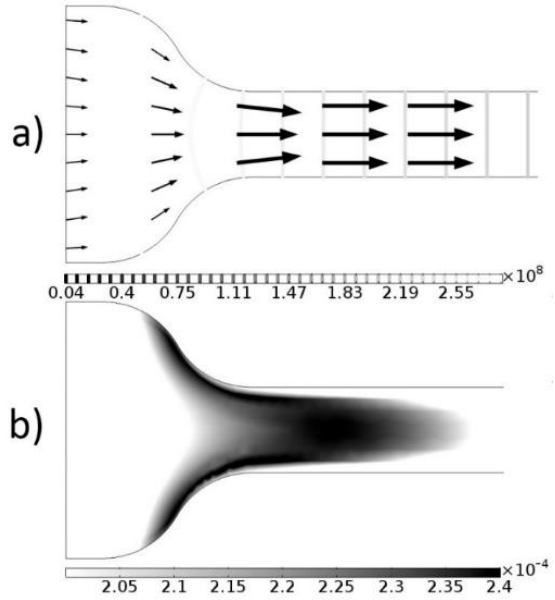

Figure 12 – Resulting solid mineral concentration showing the typical crescent-like shape of the rollfront, with lines representing flow velocity: a) velocity, b) concentration

Numerical simulations were conducted using different channel geometries, including widening (Figure 13) and a channel with a narrow section (Figure 14), to analyze the pressure field and solid mineral concentration. In all these cases, a crescent-shaped front was observed. Even after the pressure distribution became more uniform, the concentration front did not fully regain its original shape. This can be attributed to the low concentration of oxygen during the experiment, which may have limited the redeposition of significant amounts of minerals further downstream within the relatively short duration of time.

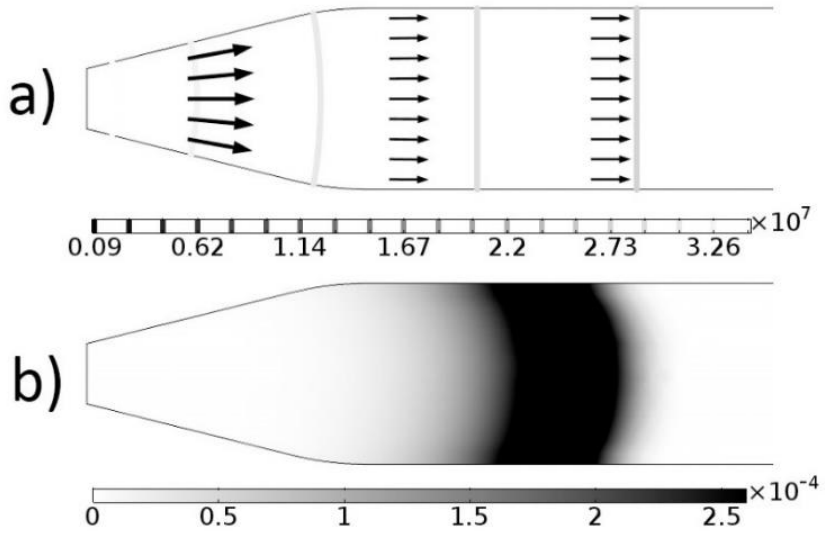

Figure 13 – Crescent shape resulting even from the channel's expansion

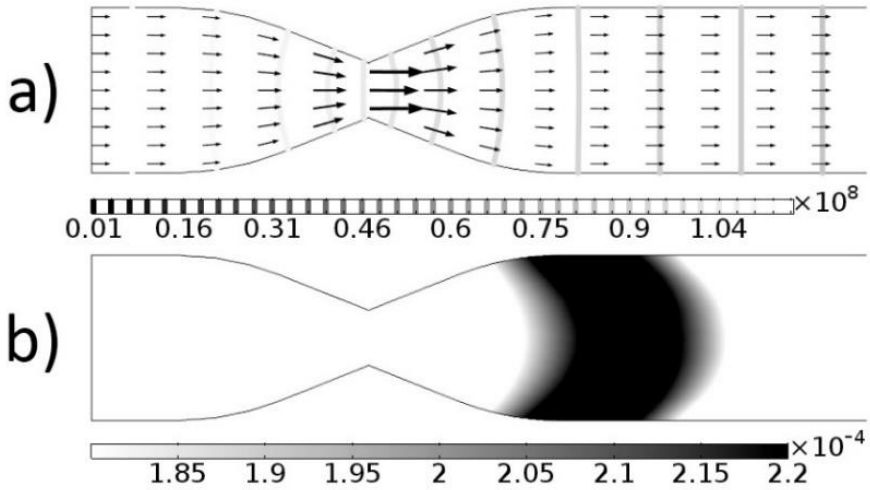

Figure 14 – Crescent shaped rollfront after constriction and then expansion of the channel

According to Brovin a phenomenon of dissolved uranium slipping through a reductant zone and precipitating further downstream in another reduced regions has been observed in geological observations [12]. To replicate these conditions, numerical simulations were conducted by introducing two reductant zones within the same channel as depicted in Figure 15. In this scenario, two rollfronts can simultaneously form within the same horizon. The minerals will migrate towards the downstream reductant zone when the concentration of reductant in the upstream zone is depleted.

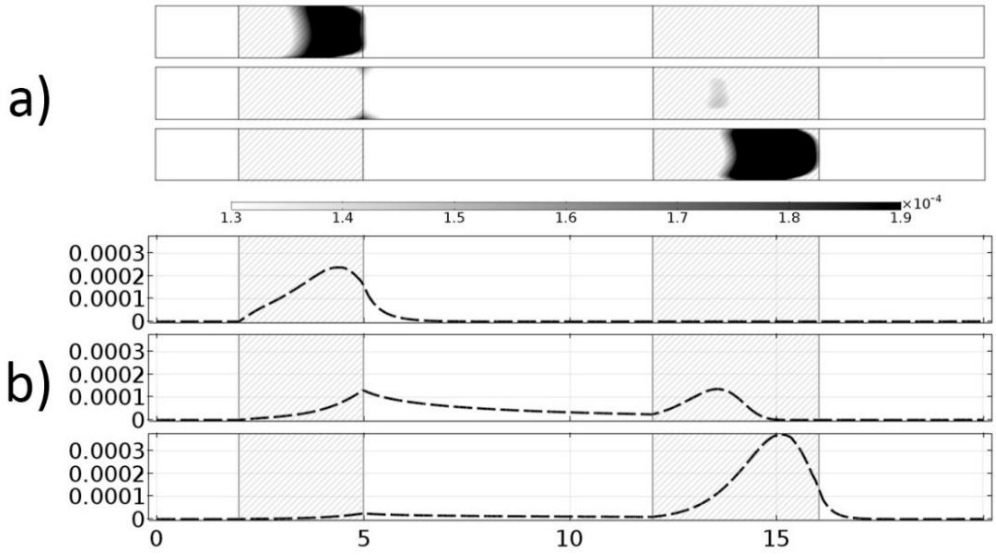

Figure 15 – Uranium concentration moving from one reduced zone to another. a) 2D solid uranium concentration. b) 1D solid uranium concentration.

Numerical simulations have shown that the velocity of rollfront movement has a somewhat linear dependence on groundwater flow velocity, as depicted in Figure 16. This linear relationship holds true for different concentrations of reductant, as

demonstrated in Figure 17. Therefore, it can be inferred that the ratio of the rollfront velocity to the groundwater flow velocity remains constant. For example, when the oxidant concentration is 0.02 $g \cdot l^{-1}$ and the reductant concentration is 0.8 $g \cdot l^{-1}$, the velocity of rollfront re-deposition is 240 times slower than the velocity of the groundwater flow, as illustrated in Figure 17.

In the Chu-Sarysu basin (Kazakhstan), the rollfront deposits are located approximately 600 km away from the hypothesized source of leached uranium in the Tianshian Mountains, as shown in Figure 18. This implies that the dissolved uranium has traveled through unconsolidated sands to its current location over a distance of around 600 kilometers.

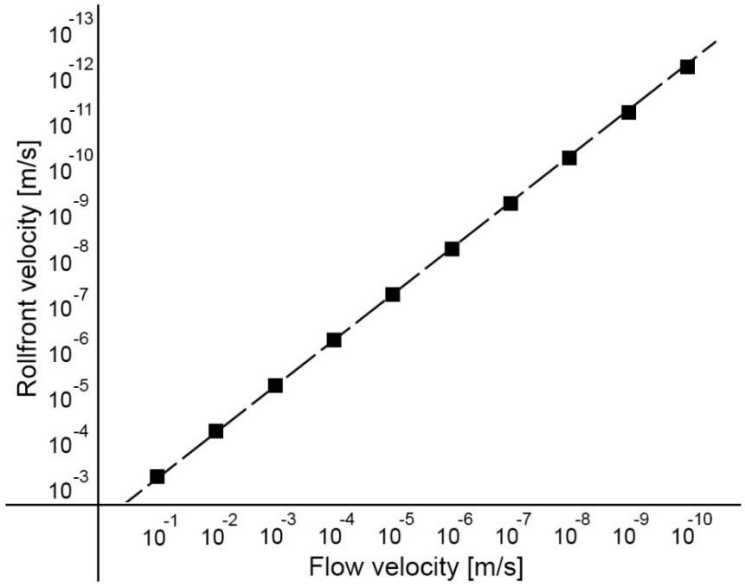

Figure 16 – Flow velocity of groundwater versus rollfront velocity at reductant concentration 0.8 $g \cdot l^{-1}$ and oxidant concentration 0.02 $g \cdot l^{-1}$. Both axes are in logarithmic scale

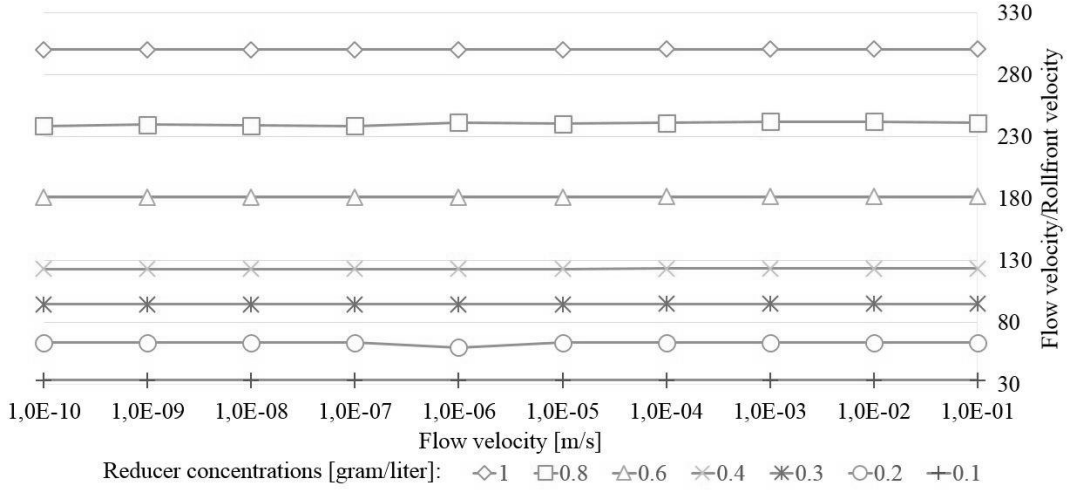

Figure 17 – Dependence between ratio of rollfront velocity over flow velocity and reducer concentration

Based on the research by Brovin et al. [12], the average filtration velocity of groundwater ranges from 0.8 to 1.3 m/yr (meters per year) [equivalent to about 2.5-4.4 × 10-8 m/s]. Considering this range of groundwater flow velocities, it would take approximately 111 to 180 million years (M.yr) for the rollfront to travel the distance between the source and the Chu-Sarysu basin, assuming that a highly reducing environment and oxidant are maintained. The uplift of the Tianshian Mountains, which led to the leaching and deposition of uranium in the basin, occurred around 23-33 million years ago [28]. This suggests that the average initial concentration of reducing agents along the flow path would have been approximately 0.16 grams per liter.

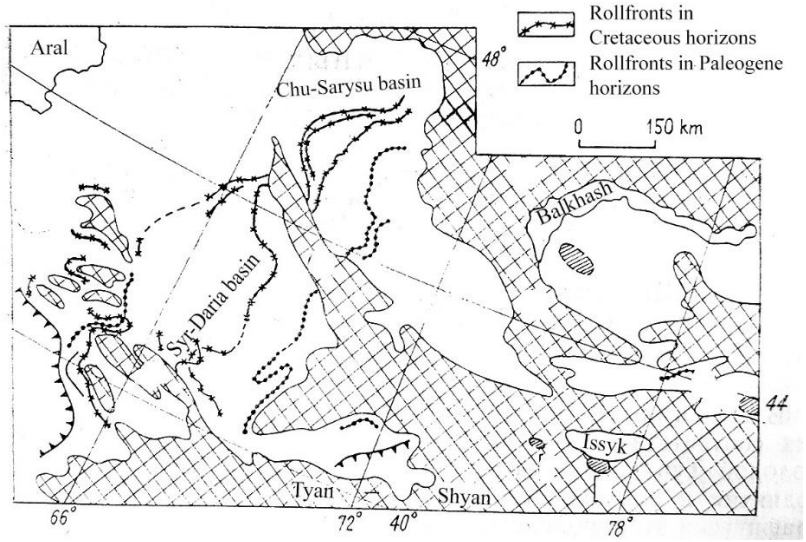

Figure 18 – Map depicting the geology of Chu-Sarysu and Syr-Dariya provinces along with discovered rollfront uranium deposits [12]

The formation of roll-shaped deposits in sandstone uranium deposits is clearly influenced by changes in the geometry of the permeable formations. Numerical simulations demonstrate that both constrictions and expansions of the permeable channels lead to the formation of crescent-shaped deposits.

The main mechanisms contributing to rollfront formation are convection and chemical reactions during uranium precipitation and dissolution. Convection is influenced by factors such as pressure differences resulting from geological inclination, channel geometry, and filtration properties. Reactions, on the other hand, depend on the properties of specific chemical complexes involved in rollfront formation.

One of the challenges in current modeling of rollfront deposits lies in the unknown reaction coefficients between solutions containing dissolved minerals and the reducing environment. These coefficients need to be determined through laboratory experiments specific to each deposit. The rate of the reaction plays a crucial role in determining the extent to which solid minerals spread along the streamlines. Other factors controlling the migration distances of minerals in reduced sandstones include reductant and dissolved mineral concentrations. Insufficient values for these

parameters limit the spread of uranium precipitation, resulting in longer migration distances before crystallization occurs.

By observing the linear relationship between flow velocity and rollfront velocity in numerical experiments, it may be possible to predict reducer concentrations or determine potential locations of rollfront deposits on a larger scale.

The model has been used to generate synthetic data for deposits formed through mineral infiltration in porous media and redox chemical reactions. This data can be used to test and validate modeling techniques based on non-deterministic approaches. Additionally, the model can enhance existing stochastic modeling methods by providing additional input data based on the results of reactive transport simulations.

2 DEVELOPMENT OF STREAMLINES BASED STOCHASTIC METHOD FOR RESOURCE ESTIMATION OF ROLLFRONT DEPOSITS

Previous studies have explored stochastic simulations to analyze the distribution of ore grades within roll-front type deposits and to understand the geological processes involved in their formation. Research described in this chapter suggests certain modifications and enhancements to conventional geostatistical algorithms to better capture the hydrodynamic constraints that govern fluid flows in ore-bearing layers.

One specific improvement proposed is to incorporate the time of flight (TOF) of water particles along the streamlines, along with available well data, when calculating the variogram. This approach departs from the traditional use of Euclidean or curvilinear distances and instead considers the TOF, leading to more accurate interpolation results and resource estimation for rollfront deposits.

Non-deterministic streamline-based methods show promise in providing more accurate interpolation results and resource estimation compared to traditional geostatistical approaches when applied to rollfront deposits. The results provided in this chapter confirm this. These modifications aim to better account for the unique characteristics and constraints associated with fluid flow in these types of deposits.

2.1 Synthetic deposit generation

Research described in previous chapter has been leveraged to utilize a simplified model of rollfront genesis, aiming to generate a realistic spatial distribution of uranium deposits, in which numerical experiments identified reaction rate constants based on available empirical experimental data. The only reliable way to verify the reliability of any geostatistical method is to conduct an MRI scan of underground stratum, which is impossible for obvious reasons, hence one way of conducting verification of prospective geological modeling methods is to utilize a synthetic deposit. The model developed in previous chapter was utilized to create a synthetic deposit.

The domain under consideration has dimensions $270 \times 450 \times 60$ m. A solution containing dissolved uranium together with an oxidant (O_2) are injected from one side into a box shaped domain (Figure 19). Solution enters the box from one side (inlet), reacts with the compounds inside, and exits from the opposing side (outlet), while the other lateral sides of the box are regarded as impermeable.

The process of simulating the synthetic rollfront deposit involves several steps. Initially, a non-uniform distribution of filtration coefficient is generated throughout the calculation grid within the domain. Continuous delivery of oxygen and uranium is then initiated until the maximum uranium concentration reaches levels comparable to those found in real deposits (0.03% [15]). Once the desired concentration is attained, uranium delivery is halted, allowing the mineral concentration to redistribute, accumulate, and form a roll-front shape downstream. The model to generate a synthetic deposit conformed to the assumptions made in previous chapter.

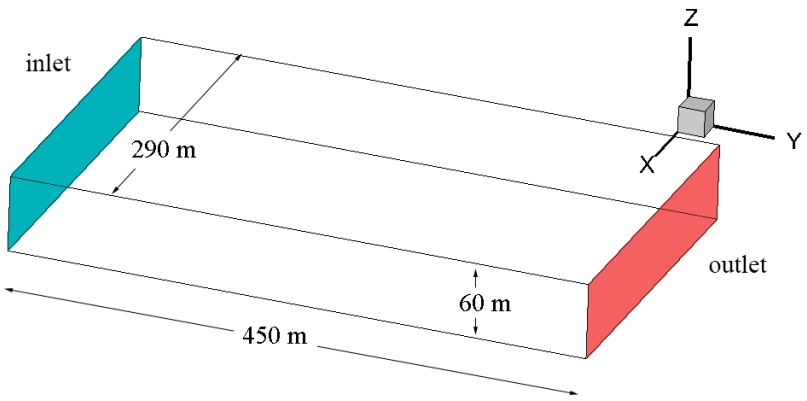

Figure 19 – Simulation domain with green side being solution inflow section, while red side depicts outflow section

Initially, the initial permeability distribution was established as idealistic and heterogeneous (Figure 20) to induce the distinct sinusoidal shape of the deposit.

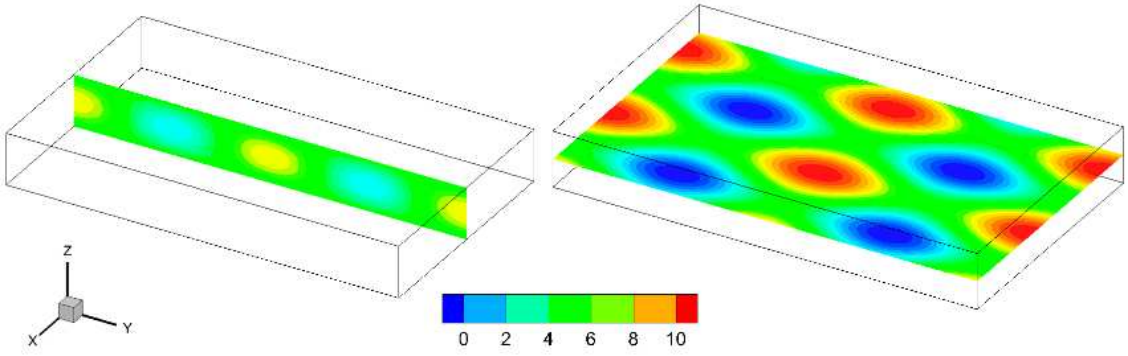

Figure 20 – Idealized permeability distribution expressed in meters per day

The pressure boundary conditions were set as no-flow along the lateral boundaries of the domain. Moreover, on the inflow and outflow conditions were determined by the hydraulic head difference, with the requirement that the height difference between the inlet and outlet be 2 m (Figure 21). Abundant reductant is assumed throughout the domain.

Except for the reductant, all concentrations within the domain were initially set to zero. During the simulation, dissolved mineral concentrations were reset to zero once they reached the desired maximum concentration of 0.03%, typically regarded as economically exploitable. That is, the inflow of uranium-rich solutions ceases once concentrations similar to those observed in real-world deposits are reached.

Consequently, synthetic three-dimensional models of roll-front deposits were generated for the purposes of verification and comparison of geostatistical methods (Figures 4 and 5).

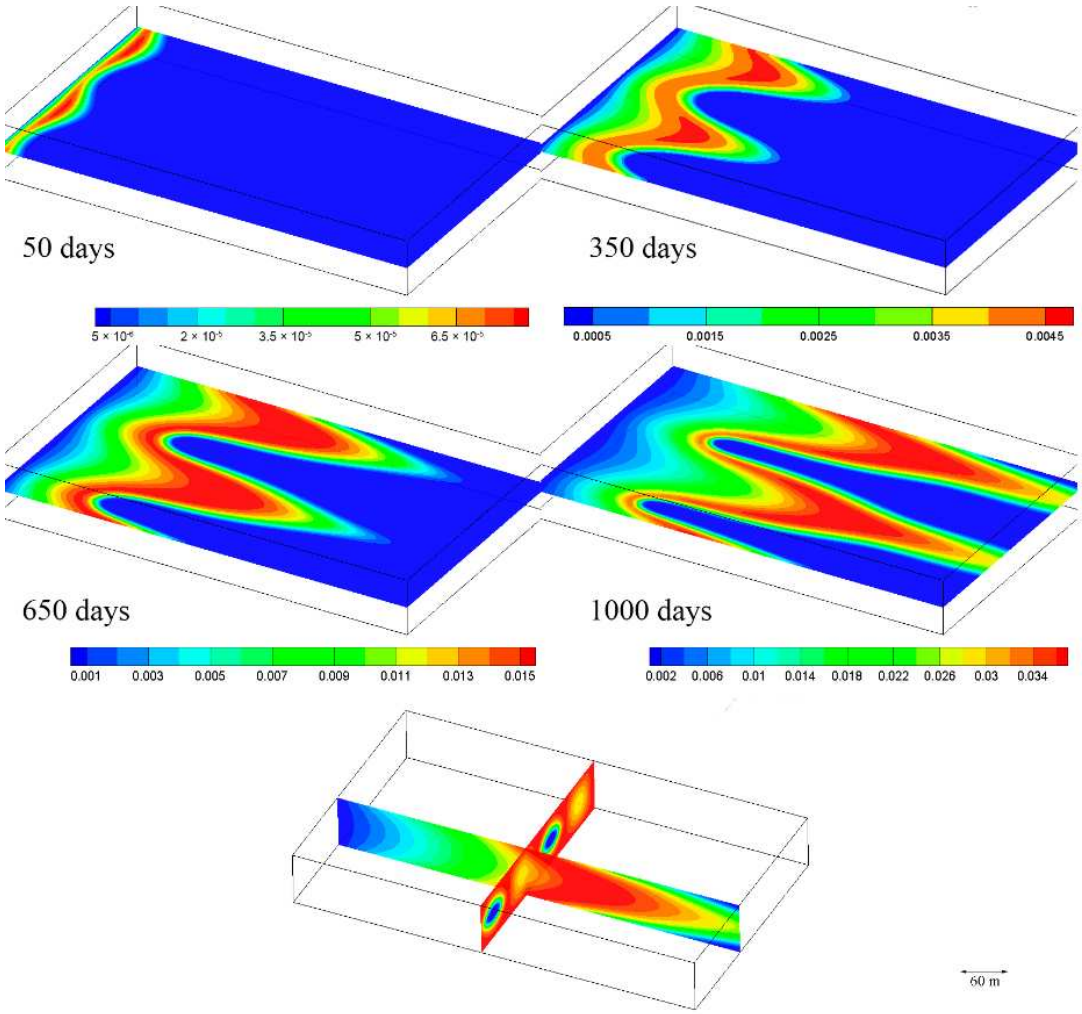

Figure 21 – Z-axis slice illustrating the variation in solid mineral concentration over a span of 1000 simulated days (approximately less than 3 years) with a legend varying in percentage to depict low concentrations at the initial stage

The idealized filtration distribution is evidently not reflective of conditions observed in real-world deposits. Consequently, additional simulations were performed using a domain characterized by filtration property distributions obtained from a genuine deposit located in Southern Kazakhstan to produce a secondary deposit. Figure 22 illustrates the simulation process spanning 1000 days aimed at generating a synthetic deposit closely resembling a real one to the greatest extent possible.

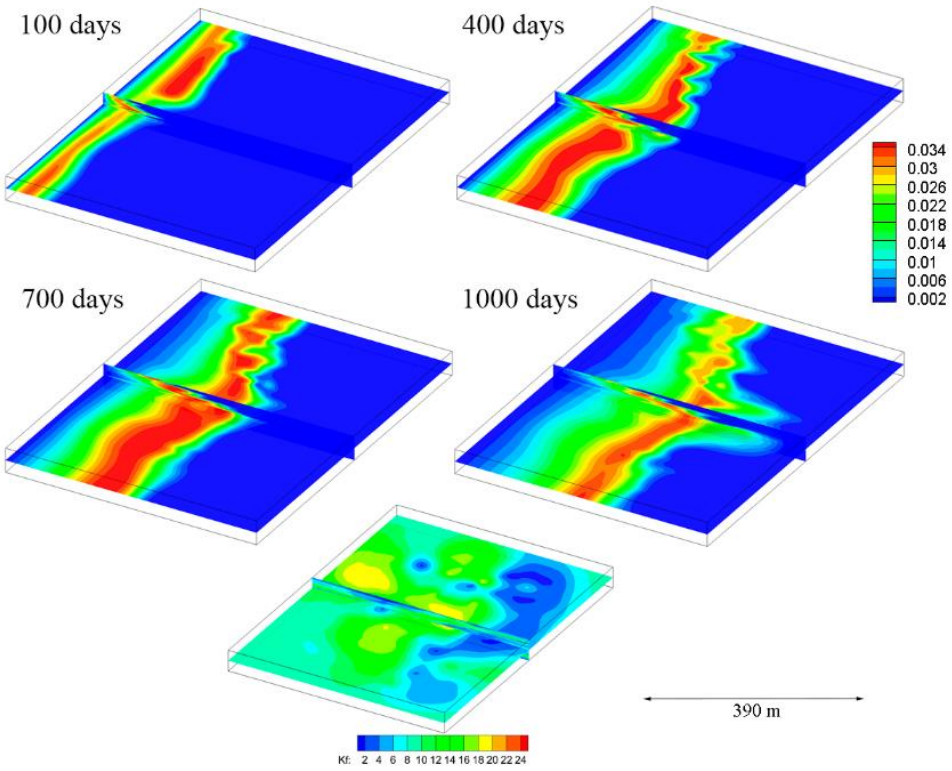

Figure 22 – The formation of the deposit over time within a heterogeneous porous medium

2.2 Streamline stochastic method and resource estimation of rollfronts

At present, geophysical well logging stands as the sole reliable method for measuring solid mineral concentrations and serves as input data for geostatistical methods. Geostatistical methods aim to ascertain the spatial distribution and concentration of minerals within the inter-well space.

Epigenetic mineral deposits, such as rollfronts, are categorized as those whose genesis occurred after the creation of the hosting environment, primarily in Eocene sandy formations, if uranium deposits located in Kazakhstan are considered. Their structural and geometric characteristics lead to the development of preferential flow pathways and finger-like patterns commonly observed in solute transport phenomena within porous media, characterized by unstable fingering fronts indicative of non-Fickian flow transport. Hence, as compared to interpolating permeability or porosity, the application of traditional stochastic methods to model infiltration-type uranium deposits becomes more challenging due to the absence of clear horizontal anisotropy inherent in sedimentary rocks.

Several geostatistical methodologies have been explored for modeling uranium-containing rollfront deposits [14, 36, 37]. Recently, a 3D modeling technique based on the principles of "Pluri-Gaussian Simulation" has been adopted [38]. Conventional methods are inherently subjective, with uncertain estimations, prompting many geostatistical approaches to resort to pluri-gaussian simulation methods [38], wherein the most probable model is selected from numerous simulations. The epigenetic nature of roll-front genesis contributes to the irregular distribution of uranium grades,

resulting in complex concentration geometries that further complicate the resource estimation process. This complexity often results in noisy variograms, which are typically addressed through Gaussian transformations [36].

The nature of roll-front formation is dictated by the hydrodynamics of infiltration process. Intuitively, accounting for the hydrodynamic properties of the stratum in geostatistical calculation should increase the accuracy of geomodelling processes.

The proposed methodology employed in this study relies on streamlines computed from filtration velocity vectors. Streamlines represent a series of curves that depict the trajectory of particles tangent to the flow velocity vectors within a specified domain. Streamlines have been extensively utilized in multi-phase flow transport modeling within oil and gas reservoirs since the 2000s [39–42], although their application in mineral resource contexts has been relatively limited according to existing literature. Parametrizing the streamlines by their proper time, known as the time of flight (TOF), is a classical approach. TOF is defined as the time required by a fluid molecule to travel from the injection point through the medium along the streamline.

In the context of resource estimation and geomodelling of deposits, the fundamental equation of an estimation-type geostatistical method involves assigning weights to hard data points (observations from wells) with known concentration values. These weights are then used to estimate the concentration at a point of interest:

$$Z^*(x) = \sum_{i=1}^{n} \lambda_i \mathrm{Z}(x_i) \tag{22}$$

where

x_i – is the location of a known data point i,

$\mathrm{Z}(x_i)$ – is concentration of component at the point x_i,

λ_i – the weight assigned to concentration at point i,

$\mathrm{Z}^*(x)$ – is the concentration value at any random point located at position x.

The selected algorithm for determining and assigning weights to hard data points significantly impacts the accuracy of the method under consideration. Inverse distance methods utilize specific coefficients to establish the exponential correlation curve over distance, with a typical formula to determine weight taking the following form:

$$\lambda_i = \frac{\frac{1}{d_i^p}}{\sum_i^n \frac{1}{d_i^p}} \tag{23}$$

where

d – is distance between the point of interest to a point with known data I,

p – is some subjective coefficient assigned by geologists.

The anisotropy is honored by the following formula:

$$\mathrm{d_i} = \sqrt{a(x - x_i)^2 + b(y - y_i)^2 + c(z - z_i)^2} \tag{24}$$

where
a, b and c – are anisotropy coefficients for directions x, y and z respectively:

In kriging-based methods a variogram function is calculated over a given hard data.

$$\gamma(h) = \frac{1}{N(h)} \sum_{N(h)} E[Z(x + h) - Z(x)]^2 \tag{25}$$

where
h – distance between points of interest,
$N(h)$ - number of points at distance equal approximately to h.
As evident, these algorithms heavily rely on distances between points.
The objective of the research in this section is to modify the ordinary kriging algorithm, incorporating streamlines as guiding paths to identify influencing nodes and compute time of flight along these nodes for weight assignment. Put differently, the streamline-based kriging method represents an ordinary kriging approach within a Riemannian or non-Euclidean space, where distances are determined by the time of flight (TOF) computed along the streamlines (days necessary to reach a certain point along the streamline). Streamline-based Kriging interpolation will involve the following procedures:

1) generating streamlines within the medium by solving the flow equation;
2) employing TOF as substitute to distances for Kriging computations;
3) performing classical calculations using the conventional kriging algorithm, albeit with TOF distance (flow time difference) rather than Euclidean distance (Figure 23).

To establish a grid based on streamlines, the following steps are required:

1) computing the hydraulic head field using filtration properties obtained from hard data;
2) determining the velocity field according to Darcy's Law and constructing streamlines;
3) estimating the time of flight along the streamlines.

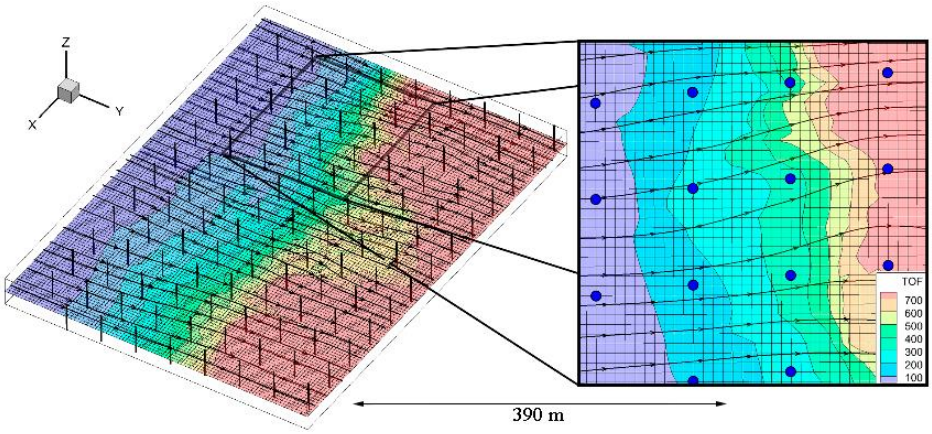

Figure 22 – Calculated streamlines and value of TOF throughout the domain.

The hydraulic head field is computed by considering the known distance between the inflow and outflow sides of the geological block in question, alongside the average permeability and groundwater velocity. Conversely, the velocity field is determined through application of Darcy's Law and the incompressible continuity equation:

$$\begin{gathered} \Delta H = -\frac{v_{avg}\Delta L}{k_{avg}}, \\ \bar{v} = -k_f \overrightarrow{\text{grad}}(H), \\ \text{div}(\bar{v}) = 0 \end{gathered} \tag{26}$$

where

ΔH – hydraulic head difference [m],

v_{avg} – average filtration velocity [m/s],

k_{avg} – average hydraulic conductivity [m/s],

$\bar{v}$ – velocity [m/s],

k_f – hydraulic conductivity determined for each point of the domain through well-log data and interpolation.

The hydraulic field is established using the following equation:

$$\text{div}(k_f \overrightarrow{\text{grad}}(H)) = 0 \tag{27}$$

Streamlines are computed utilizing Pollock's method [46], employing a technique proposed in [47]. Initially, this process is applied to each known hard data point, from well-log data, along each well, and subsequently to each node in the grid. Following this, the time of flight is calculated for each streamline. A crucial concern is ensuring that each streamline intersects a hard data point, a task that proves challenging, especially when the starting point for each streamline is assigned to the

inflow side of the domain. Under such circumstances, streamlines are highly likely to bifurcate or converge along the iso-pressure surfaces. To address this issue, we opt to designate the starting point for each streamline at each hard data point along the well, initially downstream. Subsequently, we implement a reverse upstream tracking algorithm. The downstream and upstream streamlines are combined, and subsequently, the time of flight is recalculated as shown on Figure 23.

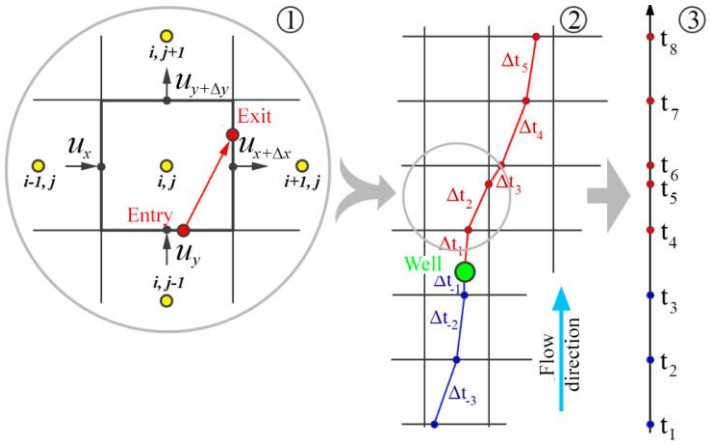

Figure 23 – (1) The computation of streamlines following Pollock's methodology; (2) calculation of streamlines both downstream and upstream from exploratory well; (3) streamlines merging to recalculate TOF

This procedure can be applied to every node within the source grid. Due to variations in the velocity field, derived from the hydraulic head field influenced by the assigned permeability of the domain, identical time of flight values may occur at different distances along the streamlines. Connecting points along each streamline with equivalent time of flight values enables the creation of a structured curved grid that conforms to the hydrodynamic characteristics of the domain (refer to Figure 24). This deformed non-Euclidean 2D or 3D space will be utilized for calculating distances required for variogram estimation or conducting kriging analyses.

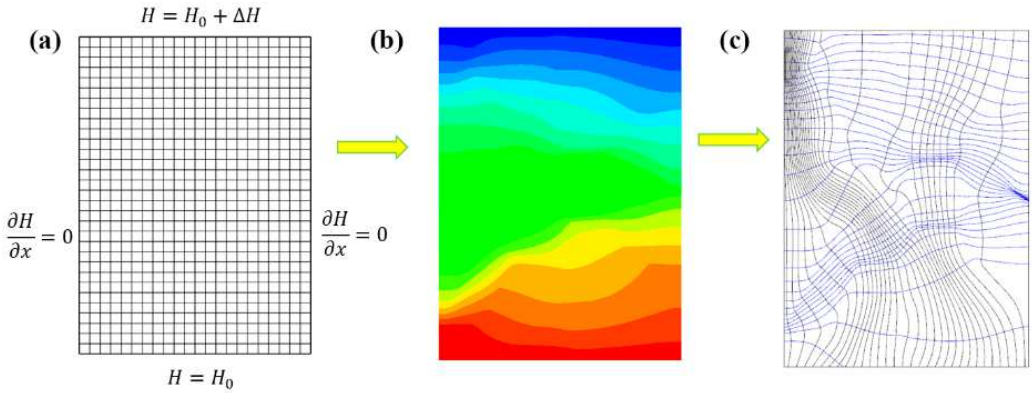

Figure 24 – (a) Initial grid; (b) hydraulic head field; (c) streamlines and orthogonal iso-surfaces of time of flight

In the traditional method, iteratively, for every point where an estimation or simulation is conducted, a collection of hard data points is assembled within the radius of a search ellipsoid. The shape of this ellipsoid is determined by a chosen anisotropy, as depicted in Figure 25.

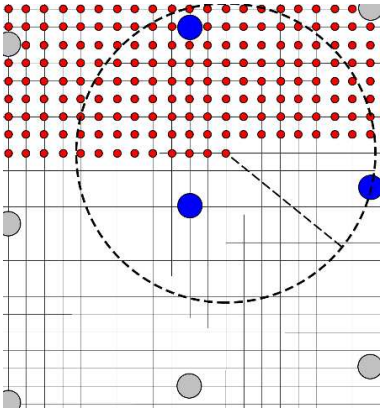

Figure 24 – Conventional identification of influential points according to the Kriging algorithm (no anisotropy)

In the proposed methodology, a comparable procedure is implemented for every node within the domain under examination. Nonetheless, the search is conducted based on the difference in TOF values and along the computed streamlines as shown in Figure 25. The premise is that, owing to the epigenetic and hydrodynamic characteristics of deposit genesis, points linked by streamlines, or in close proximity along a streamline, are expected to exert greater influence in the estimation process. Put differently, two points are considered proximate if they are linked by a groundwater flow streamline, and their separation is proportional to the difference in their TOF values.

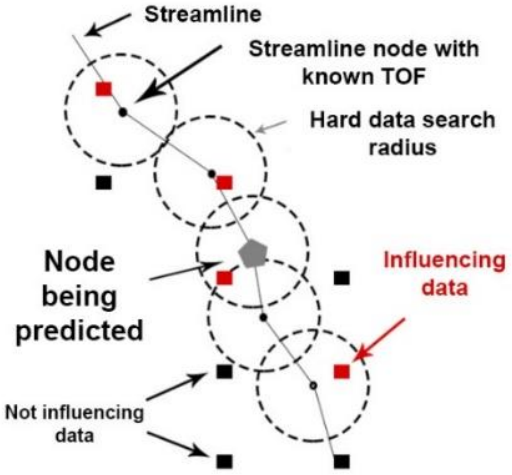

Figure 25 – The time of flight allocated to hard data identified along the streamline serves as a distance parameter for variogram calculation, while influential points are found within a specified time of flight distance from the streamline

This search domain can be visualized as a stream tube following the streamline with a chosen radius, resembling the Kriging algorithm but employing TOF. The variogram function will now have a different form:

$$\gamma(l) = \frac{1}{\mathrm{N}(l)} \sum_{\mathrm{N}(l)} \mathrm{E}[\mathrm{Z}(\tau(x) + l) - \mathrm{Z}(\tau(x))]^2 \tag{28}$$

where

$\gamma(l)$ – is a variogram at the TOF distance l,

$N(l)$ – is the quantity of nodes separated by a time difference l,

$\tau(x)$ – represents the time of flight of node x along a streamline passing through this point.

For each hard data node discovered along the streamline, weights are computed as:

$$\lambda_i = \frac{\mathrm{C}(\tau(x_i))}{\sum_{j=1}^{n} \mathrm{C}(\tau(x_j))} \tag{29}$$

where

C – is a covariogram calculates as $C(l) = \sigma^2 - \gamma(l)$, while a variance $\sigma^2(x)$ is given for each estimate $Z^*(x)$.

A series of exploratory wells are "drilled" into a previously generated synthetic rollfront deposit to assess the proposed method as shown in Figure 26. Hard data is gathered from each well and employed as input data for the method. The actual grade distribution within an exploited ore deposit will serve to estimate the error associated with the proposed method.

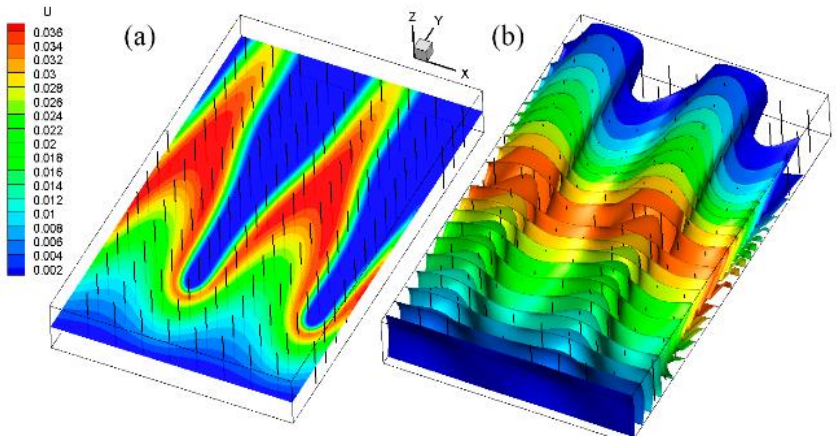

Figure 26 – Exploratory wells are drilled into a synthetic deposit: (a) horizontal slice via z-axis; (b) iso-surfaces by hydraulic head values in 3D

Conventional kriging is employed to assign permeability values to the nodes utilizing well log data. Subsequently, the hydraulic head field, velocity field, and resultant streamlines are computed within the domain, relying on the filtration properties of the stratum, typically with a thickness of around 40 m (refer to Figure 27).

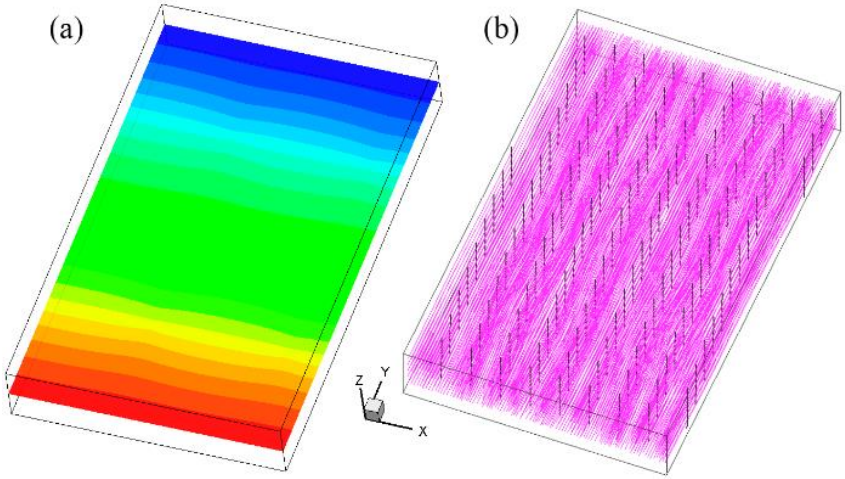

Figure 27 – (a) Hydraulic head and (b) streamlines

The uranium distribution resulting from streamline-based interpolation of well data, alongside the outcomes of ordinary kriging interpolation conducted using the SGeMS software, are depicted in Figure 28.

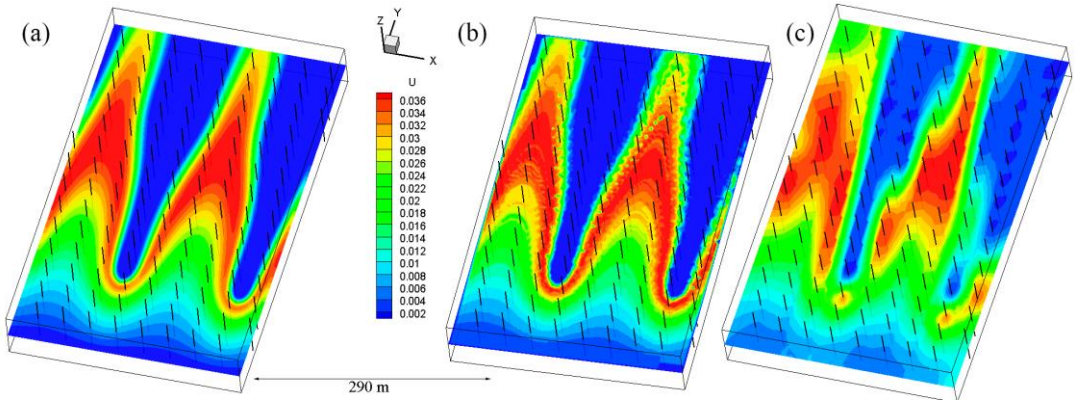

Figure 28 – Interpolation outcomes depicting (a) the true synthetic deposit, (b) streamline-based interpolation, and (c) ordinary kriging-based interpolation using SGeMS software

A synthetic deposit was created utilizing filtration data obtained from a genuine geological block within a rollfront type deposit situated in Southern Kazakhstan. The outcomes derived from employing both the streamline-based stochastic method and conventional kriging are illustrated in Figure 29.

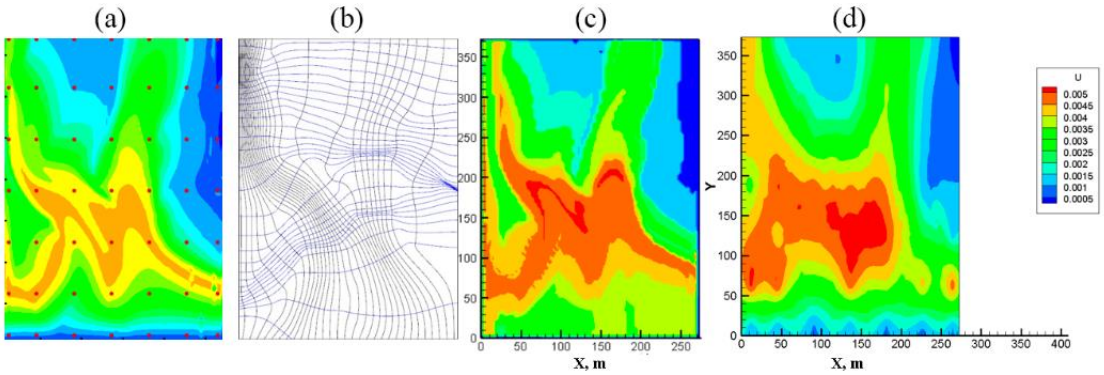

Figure 29 – Interpolation outcomes derived from actual filtration data, showcasing (a) the synthetic deposit, (b) the grid constructed using streamlines and time of flight, (c) streamline-based interpolation, and (d) ordinary kriging-based interpolation conducted with SGeMS software

It is possible to estimate the resources based on the following formula given the known concentrations for each node, along with the known density and porosity of the ore:

$$M = \sum_i \frac{C_i}{100} \rho V_i (1 - \theta) \tag{30}$$

where

M – is the total resources in kilograms,

C_i – is the concentration (in percent %) of uranium in node i,

ρ – is the density of the ore, taken at 1,700 kg.m^{-3},

θ – is the porosity, and

V_i – is the volume of a node i.

Figure 30 provides a comparison of the resource estimations acquired through classical kriging against those obtained using the proposed streamline method. Two distinct estimations were undertaken: the total resources, and the so-called “balanced” resources, wherein only nodes with concentrations deemed profitable for extraction (usually defined as exceeding 0.03%) were considered. This approach is adopted due to the primary concentration of resources occurring at the rollfront line itself, with "unbalanced" ore containing low concentrations typically regarded as unprofitable and thus excluded from the resources [15].

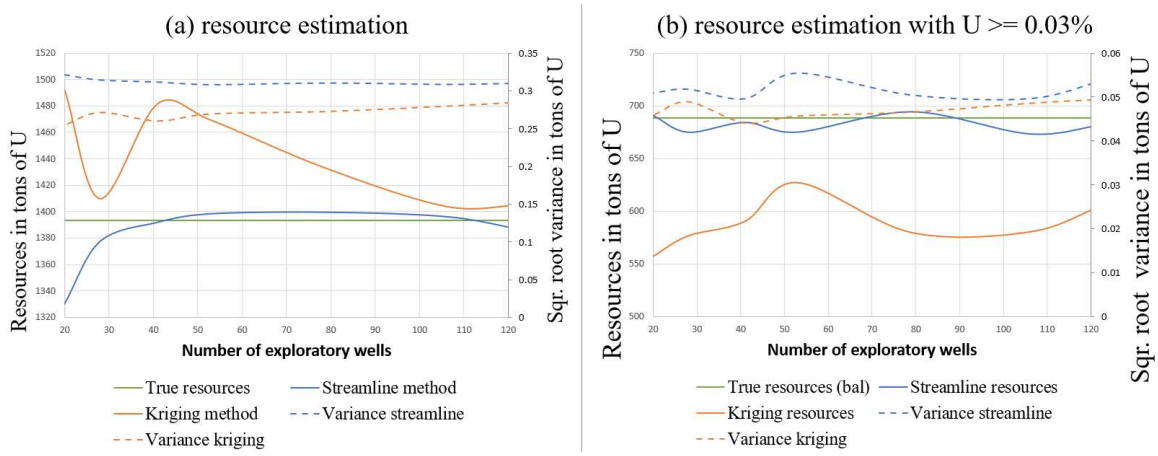

Figure 30 – The comparison of resource estimation (on the left vertical axis) and the square root of dispersion variance (on the right vertical axis) between the streamline-based stochastic method and ordinary kriging is illustrated, which includes (a) the total In-Situ resources in tons from all nodes and (b) the recoverable resources in tons with a concentration higher than 0.03%

The total uranium resources within the studied domain amount to 1393 tons, while the resources deemed profitable for extraction (defined as uranium concentrations exceeding 0.03%) are less than 688 tons. In the former case, the kriging method notably overestimated the uranium resources, whereas in the latter case, it underestimated the total mineral content of the deposit. In both scenarios, the streamline method demonstrated higher accuracy compared to kriging. For a specific case involving 80 exploratory wells, the streamline-based stochastic method estimated 694.10 ± 0.05 tons of uranium, whereas ordinary kriging computed 579.77 ± 0.05 tons of uranium. The ordinary kriging algorithm exhibited a notable enhancement with an increase in the number of exploratory wells, whereas the streamline-based approach displayed a marked improvement in accuracy with fewer exploratory wells necessary. At 28 exploratory wells, a surge in the accuracy of conventional kriging is observed, attributed to the positioning of wells in high-grade locations.

During estimation, nodes with values below the cut-off are excluded since their concentration is insufficient to be profitable. In a specific scenario involving 53 exploratory wells, resources were estimated for various cut-off values. The grade cut-off curves, depicted in Figure 31, illustrate that both the proposed streamline and kriging methods estimate similar In-Situ reserves concerning the quantity of metal Q_U against cut-offs. Kriging appears to overestimate the reserves for small cut-offs and underestimate them for cut-offs greater than the operation cut-off at 0.3‰ U (Figure 31a), with the average grade of the produced tonnage being underestimated in every case (Figure 31b).

Figure 31 illustrates the fitting of theoretical curves for the quantity of metal(Q_U)/grade (U) vs. cut-off (c), achieved through a mean squared errors method, as described by the following equations:

Streamlines

$$Q_U(kt) = -9.7333\,c^2 + 0.5695\,c + 1.3052\ (R^2 = 0.9945)$$
$$U(‰) = -0.3621\,c^2 + 0.6143\,c + 0.195\ (R^2 = 0.9944)$$

Kriging

$$Q_U(kt) = -151.88\,c^4 + 93.325\,c^3 - 25.623\,c^2 + 0.4823\,c + 1.4891\ (R^2 = 0.9993)$$
$$U(‰) = -0.3647\,c^2 + 0.6441\,c + 0.1804\ (R^2 = 0.9977)$$

Truth

$$Q_U(kt) = -167.77\,c^4 + 98.107\,c^3 - 24.939\,c^2 + 0.8392\,c + 1.3962\ (R^2 = 0.9994)$$
$$U(‰) = -1570.2\,c^6 + 1998\,c^5 - 988.28\,c^4 + 239.56\,c^3 - 29.632\,c^2 + 2.2179\,c + 0.1723\ (R^2 = 0.9977)$$

(30)

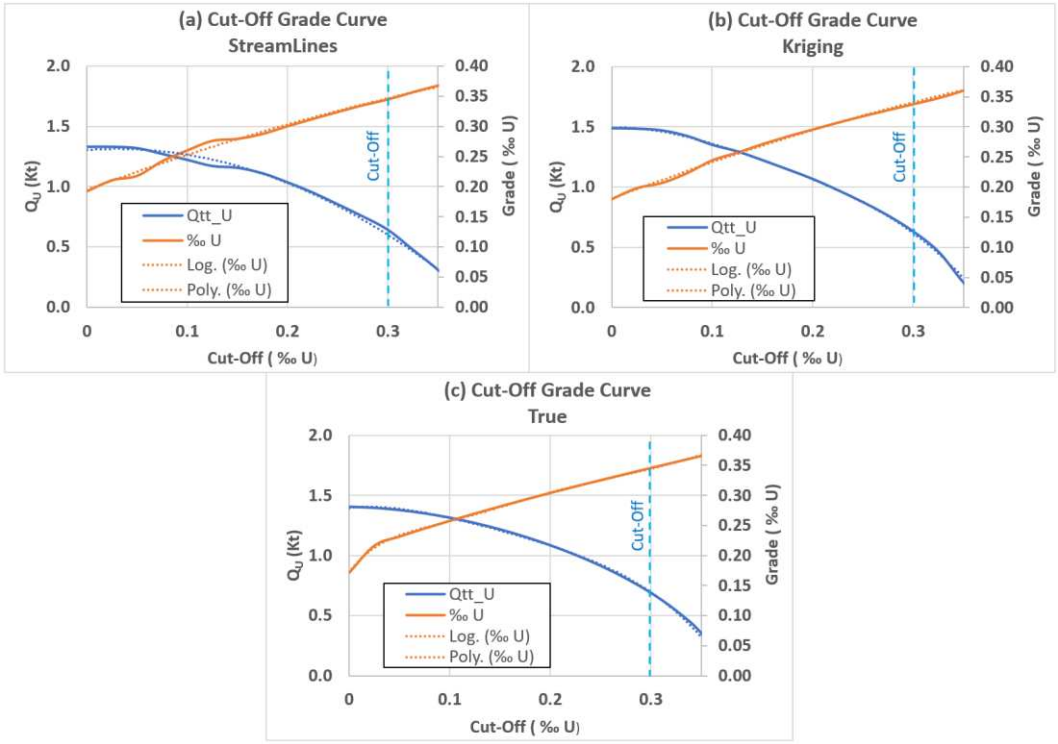

Figure 31 – Grade cut-off plots depicting resources (in blue) and grades (in orange) across cut-offs spanning from 0 to 0.35 ‰U, along with fitted trend lines (shown as dotted lines) and the exploitation cut-off set at 0.3‰U (illustrated by the blue vertical dashed line) for (a) the proposed streamline-based method, (b) the kriging method, and (c) the actual resources from the simulated deposit

In Figure 32, grade values and resource estimates for the typical scenario involving 53 exploratory wells are presented alongside uncertainty estimation bars. The error bars were computed as the absolute disparities between the estimated values and the true values on each cell, then aggregated across all cells conforming to the constraints employed to determine the cut-off curve. For lower grade cut-offs, the streamline-based method exhibits somewhat higher accuracy in both grade values and resource estimates.

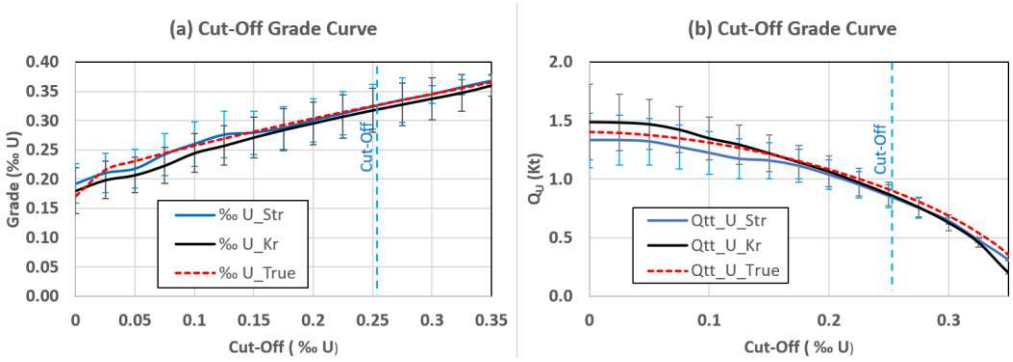

Figure 32 – Grade cut-off curves with (a) grades and uncertainty; (b) quantity of U and uncertainty for streamline-based method (blue) and kriging method (black) and synthetic deposit (red, dashed)

In regards of operational cut-off thresholds, that are usually selected as 0.3‰U at mining sites, the average grade produced is approximately 0.35‰U, which is higher. Should the mining producer's aim be to achieve an average grade of 0.3‰U, a cut-off of 0.2‰U could be preferable (Figure 31c), resulting in an increase in the metal reserves quantity from 688 to 1084 metric tons of uranium. Assuming an average price of 130 USD per metric ton, this translates to an additional in-situ value of USD 51.48 million. It is worth noting that lower cut-off grades entail increased exploitation costs due to the necessity of leaching a larger number of cells, employing a greater number of technological wells, and processing a larger volume of the solution. Nonetheless, these curves underscore the importance of investigating case-specific optimal cut-off grades according to the economic context of the deposits to maximize profitability.

The research extended beyond idealized distributions of filtration properties, encompassing an additional estimation performed on a synthetic deposit derived from data obtained from a operational field in Tukristan region, Kazakhstan. (Figure 33).

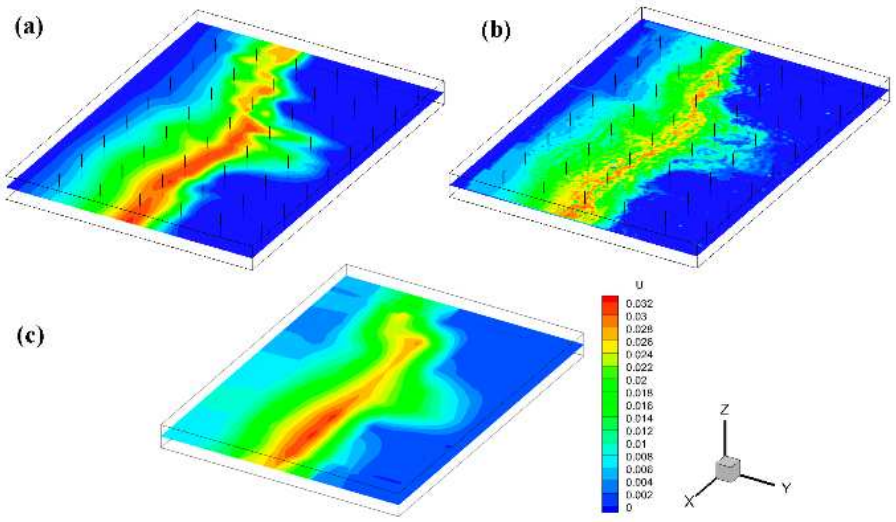

Figure 33 – Interpolation results where (a) true synthetic deposit based on real permeability data from the industry; (b) streamline-based interpolation; (c) ordinary kriging-based interpolation.

In the studied domain, with total uranium resources amounting to 357 tons with a cut-off grade of 0.03% (see Figure 34), as observed in the first scenario, the kriging method tended to overestimate uranium resources, whereas the streamline-based approach underestimated the uranium reserves. Generally, the proposed method exhibited superior accuracy compared to the conventional method. In a specific case involving 48 exploratory wells and true resources of 357 tons, streamline-based kriging estimated resources at 346 tons, while ordinary kriging estimated resources at 380 tons. Notably, the ordinary kriging algorithm displayed substantial improvement as the number of exploratory wells increased, whereas the streamline-based method demonstrated a rapid increase in accuracy with a lower number of exploratory wells.

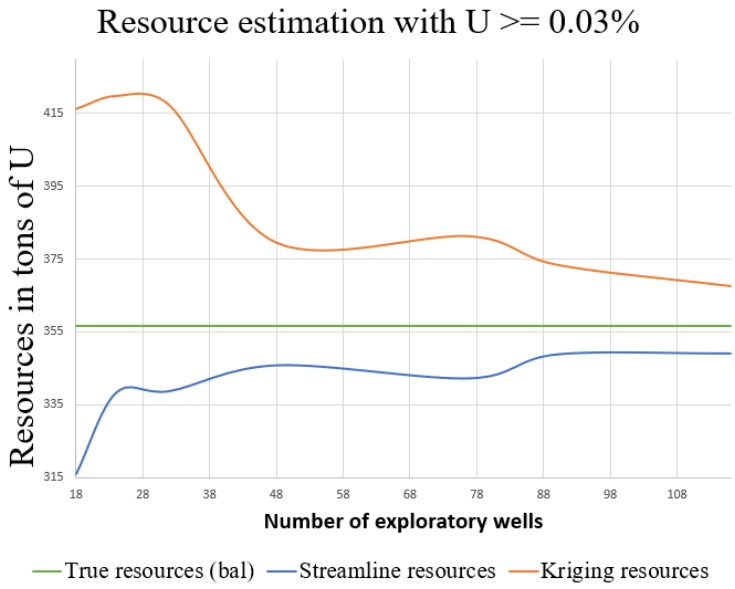

Figure 34 – Comparison in resource estimation between streamline-based stochastic method and ordinary kriging for a synthetic deposit generated based on the data from a real deposit

As can be observed the streamline-based interpolation method yields superior results in preserving the qualitative characteristics of the rollfront structure compared to the conventional kriging method, attributed to the incorporation of hydrodynamics into the interpolation.

Furthermore, for qualitative analysis, an error estimation was conducted, as illustrated in Figure 35. The maximum and average errors for each well were computed by determining the maximum disparity between values obtained from both methods and derived from the synthetic data. In quantitative terms, an increased number of wells resulted in a sharp decrease in the maximum error of the ordinary kriging, while the proposed method maintained similar estimations. Geometrically, higher maximum errors were observed in the upstream portion of the domain near the inflow side. Conversely, average errors for streamline-based kriging were lower compared to ordinary kriging across varying numbers of wells used.

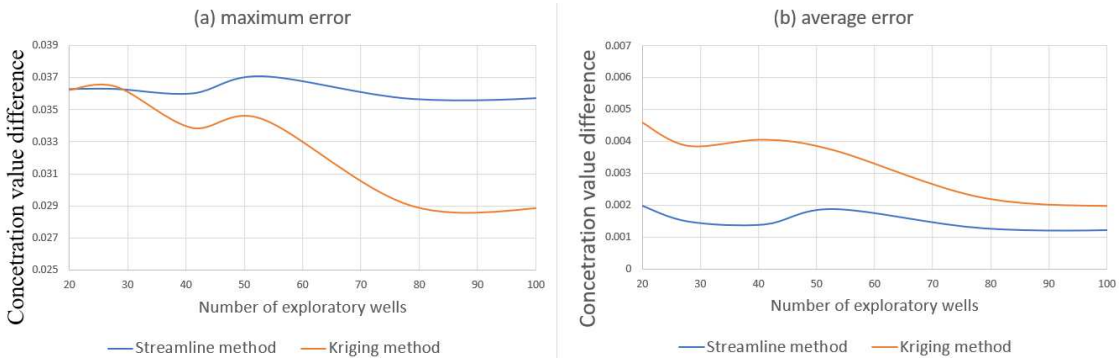

Figure 35 – Errors in resource estimation comparison between streamline-based stochastic method and ordinary kriging where (a) maximum error from all nodes; (b) average error from all nodes

The ordinary kriging algorithm, characterized by its inherent smoothness, yielded a diffusive outcome, while the streamline-based interpolation method, in certain instances, demonstrated more sharped results with improved accuracy particularly at the redox front. As depicted in Figure 35, when nodes containing mineral concentrations higher than 0.03% are considered, the streamline-based interpolation method achieves superior accuracy in resource estimation.

However, a drawback of streamline-based interpolation methods lies in the prerequisite for substantial hard data or knowledge (including geological data, permeability, etc.) of the deposit to construct a realistic flow model for computing the streamlines. Also, method relies on the assumption of a constant permeability field throughout the domain. This assumption may hold true due to the epigenetic nature of rollfront formation, whereby the hosting environment is established before the infiltration process commences. Estimating past permeability is challenging, and any discrepancies could potentially impact the estimation outcome. Variations in hydrodynamic conditions across different time periods could potentially diminish the accuracy of streamline-based kriging compared to conventional geostatistical computations. This challenge may be mitigated by incorporating additional information derived from historical data into the method.

Streamlines themselves provide additional information, that can increase the accuracy of conventional methods. Hydrodynamic conditions might have been different at various points in time, which might lead to streamline-based kriging being less accurate than ordinary geostatistical calculations. This can possibly be solved if an additional information is provided to the method itself from the available historical information.

A benefit of streamline-based methods is the ability to implement various geostatistical techniques beyond kriging, such as different simulation methods including SGS, multi-Gaussian, turning bands, etc., by utilizing the TOF rather than the traditional distance.

CONCLUSION

Brief conclusions based on the results of dissertation research.

Two significant outcomes have emerged from the research conducted within this dissertation. Firstly, a mathematical model has been developed based on empirical experimental data to simulate the rollfront genesis process. This model facilitates the identification of various mechanisms that influence the shape and composition of rollfronts from both hydrodynamic and chemical perspectives. Additionally, the model serves as a tool for generating rollfront deposits with synthetic data within a designated grid. Secondly, a novel method has been devised for geomodelling and resource estimation of epigenetic mineral deposits formed through infiltration processes.

Research has demonstrated that roll-shaped formations in sandstone uranium deposits are primarily the result of variations in the geometry of permeable formations. Numerical simulations indicate that both the constriction and expansion of these permeable channels lead to the formation of crescent-shaped deposits.

The primary mechanisms driving rollfront formation are convection and the reactions occurring during uranium precipitation and dissolution. Convection is influenced by pressure differentials resulting from geological inclinations, channel geometry, and filtration properties. The reactions are governed by the specific properties of the chemical complexes involved in the rollfront formation process.

It should be noted, however, that a significant challenge in current modeling of rollfront deposits from a reactive transport perspective lies in the unknown reaction rate coefficients between solutions containing dissolved minerals and the reducing environment. This uncertainty suggests that these parameters need to be adjusted for each specific deposit, necessitating appropriate laboratory experimentation.

Evidently, the reaction rate significantly influences the extent of solid mineral deposition along the groundwater flow direction. Other factors affecting the migration distances of minerals in reduced sandstones include the concentrations of the reductant and dissolved minerals. A deficiency in any of these parameters reduces the rate of uranium precipitation, thereby increasing the migration distance of the mineral before crystallization occurs.

Assuming a linear relationship between flow velocity and rollfront redeposition velocity, as observed in numerical experiments, it may be feasible to predict reductant concentrations (usually organics). On a larger scale, this relationship could be used to determine the probable locations of rollfront deposits.

The model derived in the first chapter has the potential to generate synthetic data for deposits formed through the infiltration of minerals via porous media and redox chemical reactions. This data can be utilized to test and validate prospective modelling techniques based on statistical approaches. Additionally, the model can be employed to improve the accuracy of existing stochastic approaches by supplying supplementary input data derived from reactive transport simulations.

A conceptually new geostatistical method, the streamline-based kriging, has been developed to account for the hydrodynamic characteristics of rollfront deposit formation. This method was tested on synthetic deposits to evaluate its qualitative and

quantitative advantages. Synthetic deposits were generated using various geometries of the underlying host environment, and stochastic methods were tested under different conditions of available well log data. Results indicate that, compared to conventional kriging estimation algorithms, the geological modeling of uranium rollfront deposits based on streamline simulation provides improved resource estimation with lower average error.

The method can be applied for an epigenetic deposit which formed through the infiltration process. Variogram calculation along the streamlines provides additional information for more precise weight assignment. Additionally, other available geostatistical methods can be amended in a similar way to account for the hydrodynamics underlying deposit genesis.

Generally speaking, the simulation methods used here to test different estimation methods have another advantage: they can be profitably used as a training simulator to teach professionals or students how to select blocks in the lixiviation technology in order to optimize the production.

Further work has to be done to verify the technique with real case deposits, as well as to modify other stochastic methods to use streamline simulation as an additional tool. This new approach opens the door for future implementations of the geostatistical simulation toolbox on non-Euclidian distance problems where distances can be deduced from the resolution of a flow transport model.

Assessing the completeness of solutions to assigned problems.

The research undertaken within current dissertation adopted a comprehensive approach, encompassing various types of studies. A literature review was conducted to evaluate the current understanding of rollfront genesis mechanisms from geological and hydrogeological perspectives. Kinetic studies of chemical processes were conducted to develop a reactive transport model capable of simulating rollfront formation process. An empirical experiment documented in the literature was utilized to ascertain reaction rates of different chemical interactions at the redox front. Building upon existing geostatistical approaches and the research findings from this study, a novel method suited for infiltration-type epigenetic deposits was proposed and tested. Consequently, the research entailed geological, hydrological, chemical, and numerical investigations, incorporating the application of geostatistics and the development of software tools.

Recommendations and source data for specific use of the results.

The research outcomes offer a multitude of applications, including the examination of rollfront genesis mechanisms at various deposit sites, the generation of synthetic data to evaluate the accuracy of geomodelling methods, the provision of training data for prospective neural network-based algorithms aimed at stimulating the In-Situ Leaching process, and the creation of a geological 3D model to estimate deposit resources based on well data.

Software modules derived from this research are currently utilized by entities engaged in uranium mining operations in Kazakhstan. Furthermore, the reactive transport model developed can be extended to encompass other elements hosted by infiltration-type deposits, such as selenium, molybdenum, rhenium, vanadium,

scandium, lithium, yttrium, and so on. Similarly, the proposed geostatistical method has potential for application beyond uranium.

Assessment of technical and economic efficiency of implementation.

Figure 34 indicates the potential positive economic impact resulting from the application of research findings derived from the present study. According to the numerical experiments conducted, the proposed method yields accurate results while requiring a substantially reduced number of exploratory wells. This reduction alone could lead to significant cost savings in well construction. Given that the capital expenditures for exploratory well construction typically range from $15,000 to $20,000 USD per well, the overall costs could be reduced by approximately $1,000,000 USD for a block that would otherwise necessitate 100 exploratory wells, now reduced to 20.

Furthermore, a more precise geological model could enhance production efficiency. Geotechnologists on-site must make informed decisions regarding technological well and well screen positioning, as well as appropriate operational regimes. These decisions rely heavily on the geological model provided by the geology department.

Some of research outcomes obtained from the current dissertation have been accomplished through grant funding projects administered by the Ministry of Science and Higher Education of Kazakhstan. These outcomes have been integrated into software modules that are actively utilized at real deposits managed by subsidiaries of the National Atomic Company JSC Kazatomprom, including LLP “Mining Company Ortalyk”, JV Inkai LLP and “Institute of Hight Technology” LLP. The author receives royalties for the developed software modules, as evidenced by the acquisition of 10 copyright certificates (№21603 dated 10.11.2021, №21602 dated 10.11.2021, №13134 dated 11.11.2020, №13055 dated 05.11.2020, №12687 dated 20.10.2020, №10493 dated 02.06.2020, №5398 dated 20.09.2019, №3695 dated 29.05.2019, №439 dated 08.11.2018, №615 dated 06.04.2017).

Assessment of the scientific level of the work performed in comparison with the best achievements in this field.

Numerous efforts have been undertaken by various researchers to identify the primary mechanisms of rollfront formations. Historically, the geology of rollfront formations has been extensively studied by many scientists, with the main principles of their genesis well-documented in Soviet and overseas literature. While the rollfront genesis process is well understood on a macro scale, few empirical experiments have been conducted to replicate this process on a smaller scale. Numerical experiments made within current work could provide valuable insights for geotechnologists involved in mining operations to facilitate optimal decision-making. The research presented in this dissertation offers a mathematical and software tool to simulate the rollfront genesis process, thereby generating data to evaluate the reliability of geomodelling methods.

Due to the intricate geometry of rollfronts, the application of conventional algorithms for accurately estimating deposit resources poses significant challenges. Consequently, leading studies in the field have concentrated on investigating methods to adapt existing geostatistical methodologies for modeling uranium-containing

rollfront deposits. Specific approaches, such as Pluri-Gaussian Simulations, have been employed to develop three-dimensional models while accommodating the complexity inherent in such deposits. However, in the present study, research has been conducted to explore the hydrodynamic and chemical aspects of rollfront genesis. The principal findings of this investigation have been leveraged to devise a new computational fluid dynamics (CFD)-based geostatistical method targeted at infiltration-type deposits.

BIBLIOGRAPHY

1. World Nuclear Association. Uranium and Nuclear Power in Kazakhstan. – London: World Nuclear Association, 2024. – 44 p.
2. Boytsov, A. Sustainable development of uranium production: status, prospects, challenges // International symposium on uranium raw material for the nuclear fuel cycle: exploration, mining, production, supply and demand, economics and environmental issues (URAM-2018). – Vienna: IAEA, 2018. – P. 49-50.
3. World Nuclear Association. Supply of Uranium. – London: World Nuclear Association, 2024. – 28 p.
4. Cameco Corp. Uranium Price. – Roswell: UxC, 2024. – 3 p. https://www.cameco.com/invest/markets/uranium-price
5. Boytsov A.V. World uranium industry: state, development prospects, challenges of the time // Proceedings of VIII International Research and Practical Conference "The topical issues of the uranium industry". – Astana, 2017. – P. 14-21.
6. OECD, NEA, IAEA. Uranium 2014: Resources, Production and Demand. – Paris: OECD Publishing, 2014. – 508 p.
7. Tarkhanov A.V., Bugriyeva E.P. The largest uranium deposits in the world / Edited by G.A. Mashkovtseva. – M.: VIMS, 2012. – 118 p.
8. World Distribution of Uranium Deposits (UDEPO) with Uranium Deposit Classification, IAEA-TECDOC-1629, International Atomic Energy Agency, Printed by the IAEA in Austria October 2009, p. 117. ISBN 978–92–0–110509–7
9. Aizhulov D., Shayakhmetov N., Kaltayev A. Quantitative Model of the Formation Mechanism of the Rollfront Uranium Deposits // Eurasian Chemico-Technological Journal. – Almaty, 2018. – V. 20. – № 3. – P. 213-221. http://dx.doi.org/10.18321/ectj724
10. Adams S.S., Cramer. R.T., Data-process-criteria model for roll-type uranium deposits, Geological environments of sandstone-type uranium deposits // Report of the working group on uranium geology organized by the International Atomic Energy Agency. – Vienna, 1985. – P. 383-399.
11. Maksimova M.F., Smariovich E.M. Stratum-infiltration ore formation. – M.: Nedra, 1993. –158 p.
12. Brovin K.G., Grabovnikov V.A., Shumilin M.V., Yazikov V.G. Forecast, prospecting, exploration and industrial evaluation of uranium deposits for mining by underground leaching. – Almaty: Gylym, 1997. – 384 p.
13. Instructions (Methodological recommendations) on underground borehole leaching of uranium. – Almaty: Kazatomprom, 2006. – 310 p.
14. Petit G., Langlais V., Khairuldin A., Fiet N., Boissezon H., Rumbach G., Oppenau T. Application of Stochastic Simulations and Quantifying Uncertainties in the Drilling of Roll Front Uranium Deposits // Geostatistics Oslo 2012. – Dordrecht: Springer, 2012. – P. 321-332. https://doi.org/10.1007/978-94-007-4153-9_26
15. Poezzhaev I.P., Panova E.N., Bulenova K.Zh., Karmanov E.M., Blynsky O.A., Bitov O.A. Geotechnology of uranium. – Almaty: NAC Kazatomprom, 2017. – 319 p.

16. Research report: Intelligent control and decision-making systems for the development of uranium and oil deposits BR05236447 (In Russian) / A. Kaltayev, M.S. Tungatarova, D.E. Aizhulov, M.B. Kurmanseiit, N.M. Shayakhmetov et al. – Almaty, 2020. – 126 p.

17. Research report: The study of the mechanisms of ore genesis and development of high accuracy digital technology to contour ore bodies in rollfront type mineral deposits AP08051929 (In Russian) / A. Kaltayev, M.S. Tungatarova, D.E. Aizhulov, M.B. Kurmanseiit, N.M. Shayakhmetov et al. – Almaty, 2022. – 126 p.

18. Research report: Development of mathematical foundations and 3D simulation model of the process of underground bacterial leaching of uranium AP09260105 (In Russian) / A. Kaltayev, M.S. Tungatarova, D.E. Aizhulov, M.B. Kurmanseiit, N.M. Shayakhmetov et al. – Almaty, 2023. – 126 p.

19. Aizhulov D., Tungatarova M., Kaltayev A. Streamlines Based Stochastic Methods and Reactive Transport Simulation Applied to Resource Estimation of Roll-Front Uranium Deposits Exploited by In-Situ Leaching // Minerals. – Basel: MDPI, 2022. – V. 12. – №10. – P. 1209. https://doi.org/10.3390/min12101209

20. Aizhulov D., Kurmanseiit M. Application of geostatistical methods for reconstruction of lithological and mineralogical structure of uranium deposit by interpolating well data // Bulletin KazNU. – Almaty, 2016. – V. 91. – № 3. – P. 45-52. https://bm.kaznu.kz/index.php/kaznu/article/view/343

21. Aizhulov D, Tungatarova M. Comparison of geostatistical methods for modeling infiltration-type uranium deposits // Bulletin KazNPU named after Abai. – Almaty, 2022. – V.79. – №3. – P. 83-90. https://doi.org/10.51889/5747.2022.61.53.010

22. Aizhulov D., Kaltayev A. Stochastic modeling of uranium roll-front deposits based on stream-line simulation // Proceedings of International Scientific and Practical Conference on “Actual Problems of Informatics, Mechanics and Robotics”. – Almaty, 2018. – P. 97-102.

23. Aizhulov D.Y., Kaltayev A. Stochastic modelling of uranium roll-front deposits based on streamline simulation // Proceedings of International symposium on uranium raw material for the nuclear fuel cycle: exploration, mining, production, supply and demand, economics and environmental issues (URAM-2018). – Vienna: IAEA, 2018. – P. 17-20.

24. Aizhulov D., Kaltayev A. Stochastic modeling of uranium roll-front deposits based on stream-line simulation // Scientific conference-seminar “Mathematics and Simulation”. – Almaty, 2018. – P. 12-17.

25. Beletskiy V.I., Bogatkov L.K., Volkov N.I., Glazunov I.S., Dolgih P.F. Handbook of Uranium Geotechnology. – M.: Energoatomizdat, 1997. – 672 p.

26. International Atomic Energy Agency. World Distribution of Uranium Deposits (UDEPO) with Uranium Deposit Classification // Nuclear Fuel Cycle and Materials. – Vienna: International Atomic Energy Agency, 2009. – 117 p.

27. Dahlkamp F. J. Uranium Deposits of the World (Asia). – Berlin: Springer-Verlag, 2009. – 492 p.

28. Dahlkamp F.J. Uranium Ore Deposits. – Berlin: Springer-Verlag, 1993. – 460 p.

29. Yazikov V.G. Features of carrying out hydrogeological and engineering - geological work at different stages of exploration and development of infiltration (hydrogenous) uranium deposits. – Tomsk: Publishing House of Tomsk Polytechnic University, 2012. – 96 p.

30. Zhivov V.L., Boytsov A.V., Shumilin M.V. Uranium. Geology, mining, economics. – M.: Atomizdat, 2012. – 304 p.

31. Boytsov V.E., Vercheba A.A. Geological and industrial types of uranium deposits: textbook. – M.: KDU, 2008. – 310 p.

32. Romberger S. B. Transport and deposition of uranium in hydrothermal systems at temperatures up to 300C: geological implications // Uranium geochemistry, mineralogy, geology, exploration and resources. – 1984. – P. 12-17. https://doi.org/10.1007/978-94-009-6060-2

33. Evseeva L. S., Ivanov K. E., Kochetkov V. I. Some laws of the formation of epigenetic uranium ores in sandstones, derived from experimental and radiochemical data // Atomnaya Energiya. – 1962. – V. 14. – P. 474-48. https://doi.org/10.1007/BF01121894

34. Bear J. Modeling Phenomena of flow and Transport in Porous Media. – Berlin: Springer, 2018. – 730 p.

35. Danaev N.T., Korsakova N.K., Penkovskij V.I. Mass transfer in the borehole zone and electromagnetic stratum well logging. – Almaty: Kazakh University, 2005. – 180 p.

36. Abzalov M., Drobov S., Gorbatenko O., Vershkov A., Bertoli O., Renard D., Beucher H. Resource estimation of in situ leach uranium projects // Applied Earth Science. – Maney Publishing, 2014. – V. 123. – № 2. – P. 71-85. https://doi.org/10.1179/1743275814Y.0000000055

37. Renard D., Beucher H. 3D Representations of a Uranium Roll-Front Deposit // Applied Earth Science. – Maney Publishing, 2012. – V. 121. – №. 2. – P. 84–88. https://doi.org/10.1179/1743275812Y.0000000011

38. Armstrong M., Galli A., Beucher H., Le Loch G., Renard D., Doligez B., Eschard R., Geffroy F. Plurigaussian Simulation in Geosciences / 2nd edition. – Berlin: Springer, 2011. – 176 p.

39. Blunt M.J., Liu K., Thiele M.R. A generalized streamline method to predict reservoir flow // Petroleum Geoscience. – 1996. – V. 2. – № 3. – P. 259–269. http://doi.org/10.1144/petgeo.2.3.259

40. Oladyshkin S., Royer J.-J., Panfilov M. Effective solution through; the streamline technique and HT-splitting for the 3D dynamic analysis of the compositional flows in oil reservoirs // Transport in Porous Media. – 2008. – T. 74. – № 3. – C. 311-329. https://doi.org/10.1007/s11242-007-9197-1

41. Thiele M.R., Batycky R.P., Fenwick D.H. Streamline simulation for modern reservoir-engineering workflows // Journal of Petroleum Technology. – 2010. – V. 62. – № 1. – P. 64-70.

42. Mathieu R., Deschamps Y., Selezneva V., Pouradier A., Brouand M., Deloule E., Boulesteix T. Key Mineralogical Characteristics of the New South Tortkuduk Uranium Roll-Front Deposits, Kazakhstan // In Proceedings of the 13th SGA Biennial Meeting. – 2015. – P. 1835-1838.

43. Pollock D.W. Semi-analytical Computation of Path Lines for Finite-Difference Models // Ground Water. – 1988. – V. 26. – №6. – P. 743-750. https://doi.org/10.1111/j.1745-6584.1988.tb00425.x

44. Kuljabekov A. Model of chemical leaching with gypsum sedimentation in porous media. Ph.D. Thesis, Univ. Lorraine, Nancy, France & Al-Farabi, Almaty, Kazakhstan. – 2014. – 111 p. https://hal.univ-lorraine.fr/tel-02075294/file/DDOC_T_2014_0369_KULJABEKOV.pdf